Structures and states
P1 Project

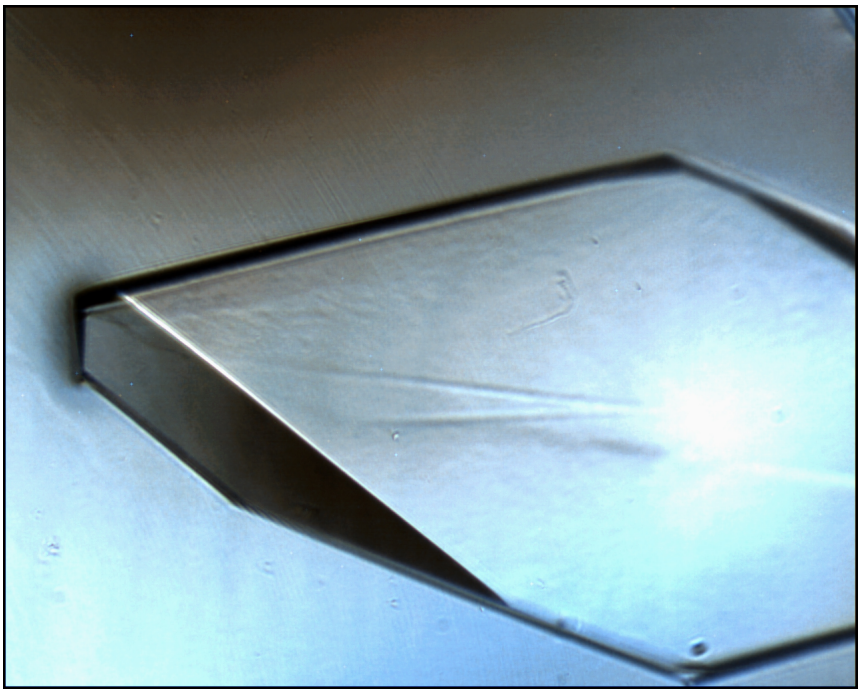

Morten V. Madsen Nikolaj L. Kildeby Ole Z. Andersen
Tom Larsen Simon C. M. Sørensen René Petersen
Rasmus E. Røge

December 20, 2004

AALBORG UNIVERSITET

Det Teknisk-Naturvidenskabelige Fakultet

Aalborg Universitet

Basisuddannelsen

TITEL:
P1 project

PROJECT PERIOD:
P1,
October 13. - December 20. 2004

PROJECT GROUP:
Nano, A307

GROUP MEMBERS:
Morten V. Madsen
Nikolaj L. Kildeby
Ole Z. Andersen
Tom Larsen
Simon C. M. Sørensen
René Petersen
Rasmus E. Røge

SUPERVISORS:
Søren Klitgaard
Lars Bo Henriksen

NUMBER OF COPIES: 14

NUMBER OF PAGES: 49

NUMBER OF APPENDICES 6

TOTAL NUMBER OF PAGES 76

SYNOPSIS:
This project is based on the initial problem: "How can different analytical techniques be used to examine molecular structures and classify different properties of these?" During the span of the project, analyzing techniques like atomic force microscopy, absorbance spectroscopy, fluorescence spectroscopy and circular dichroism has been used. On the theoretical level a description of these techniques are in the related appendices. Considerations about the setup of the equipment are described, and the experiments are discussed. The experiments include absorbance spectroscopy of $CuSO_4$ in solutions with and without NH_4. Crystals of $CuSO_4$ was examined in a microscope and studied using atomic force microscopy. A crystallized version of the enzyme lysozyme was studied in a microscope. Lastly fluorescence spectroscopy and circular dichroisme analysis of a lysozyme solution was conducted. The conclusion of the report is that there are many ways of studying nanostructures and that the problem, on this scale, is to get valid data?

Preface

This report is the product of the P1 project period on the basis year on "Aalborg University - Faculty of Engineering and Science", and it has been published by group A307. The goal of the project was to obtain knowledge about the different techniques used to analyze nanostructures. The work that makes the foundation of this report has been going on from October 13th to December 20th, 2004.

This report is for the technically interested reader with a basic knowledge of chemistry, biology and physics, and who wants to learn about the different existing techniques used to analyze nanostructures.

This report is build up of an introduction, a method description, results, a discussion of the results, a conclusion and a perspective chapter. Finally there are different appendices, which describe the techniques thoroughly and technically. There will be references from the report to appendices where appropriate.
The notation used to references sources is the Harvard method.

We would like to thank group A303, A304, A306 and A311 for letting us use their data.

Contents

Chapter 1

Introduction

1.1 Project description

This report aims to study and explain different structures and states and their influence on matter. This will be done on both organic and inorganic materials. The report will explain a variation of instruments for the study of materials. Furthermore the report will include visualization of materials in the different states. The data from the different studies of the materials will be interpreted, compared with models and discussed.

1.2 Problem analysis

Initiating problem

How can different analytical techniques be used to examine molecular structures and to classify different properties of these?

1.3 What is nanotechnology?

Nanotechnology has been described by many as the technology of tomorrow. The term nanotechnology dates back to December 29, 1959, when Richard Feynman gave his famous lecture to the American Physical Society entitled "There's Plenty of Room at the Bottom". Feynman discussed the benefits to society that would accrue if it was possible to manipulate matter and manufacture objects with precision at the scale of a few atoms across, which corresponds to a dimension of about 1 nanometer. As an example Feynman illustrated the possibility of writing the entire British Encyclopedia on a pin head by manipulating individual atoms. In context to his speech Feynman arranged a competition celebrating the first person who could achieve the goal of writing the encyclopedia on a pin head. No one has yet claimed the award, but nanotechnology has come a long way since 1959. [Encarta, 2003]

The word "nano" originates from the Greek word nânos, meaning dwarf. The definition of nano as a mathematical or physical prefix is 10^{-9}. Working with structures between 0.1 and 100 nm in size is defined as nanotechnology. As comparison, the diameters of an atom and a human hair are around 0.2 nm and 15000 nm respectively. [Lademann, 2003] Nanotechnology is a new way of science dealing with nanosized structures.

Science fiction and science

When the perspectives of nanotechnology are being discussed, the impacts of nanotechnology are often referred to. Many perceive nanotechnology almost as science fiction.

A matter of fact is, however, that nanotechnology is a wide spanning way of science. Nanotechnology combines the fields of physics, chemistry and biology with different engineering professions.

Nanotechnology in Denmark

Today Denmark holds several educations related to nanotechnology. The University of Aalborg describes nanotechnology as a way of science that enables scientists to manipulate single molecules and even atoms [AAU, 2004]. This description indicates that nanotechnology is difficult to define as one single existing subject area.

The interdisciplinary aspect of nanotechnology

Physics is an important discipline in nanotechnology because it gives an explanation to how the world functions. When something becomes smaller quantum mechanics becomes more and more important. In nanotechnology it is possible to create 2D structures, 1D structures and even 0D structures. This introduces new properties to materials and quantum mechanics is now the only way of describing the underlying physics.

Chemistry is important in nanotechnology because it provides knowledge about molecules and atoms.

Biology is important because Nature has already made nanostructures. Proteins and enzymes are a perfect example of nanostructures in real life. Basic knowledge of construction is required, as is knowledge towards electricity and more. The fact that nanotechnology combines these different areas of expertise generates certain contradictions. There are unmistakable differences between the world of physics and biology. While the focus in physics is on the theoretical level biology focuses on a more practical angle of approach. Nanotechnology can be described as a melting pot where the world of physics and chemistry meets the world of biochemistry.

Nanoscience and nanotechnology

In connection with nanotechnology there can be a long way from basic science to applied science. On a global perspective the effort in research and development in nanotechnology are distributed with 85 percent basic science and 15 percent applied science. [Nielsen, 2003].

1.4 Methods of analysing nanoscale structures

Because nanotechnology deals with structures on a scale below 100 nm the different techniques associated with normal scientific methods changes. The size of structures are shorter than the wavelength of light, hence optical microscopy is not possible.

In connection with nanotechnology different techniques for studying nanostructures exist. Among these are atomic force microscopy, X-ray diffraction, fluorescence spectroscopy, circular dichroisme and differential scanning calorimetry. A short summery of the techniques used in this project follows.

Optical microscope

An optical microscope uses light sent through lenses to create a magnified two dimensional image.

Atomic Force Microscopy

Atomic force microscopy is a method of measuring the topography of a surface using a nanoscaled pickup. In contrast to an optical microscope the atomic force microscope solely collects data about vertical levels of an area. More information about the subject can be found in Appendix C .

Absorption Spectroscopy

Using this technique it is possible to determine at which wavelengths a sample absorbs light. This information can be used to find the concentration of a sample. The loss of intensity is measured after the sample has been illuminated. For instance, a light source with a wide band of wavelengths can be directed at a sample. The particles will absorb those wavelengths, which can excite them from one quantum state to another, see Section 1.9 . After the light has passed through the sample, the intensity of the absorbed wavelengths will be reduced compared to the original light spectrum. See Appendix C.2 for more information.

Visualization

Visualization can be a result of x-ray diffraction. It is not a technique, but it enables scientists to visualize different proteins. Data from X-ray diffraction reveals the position of the individual atoms in a protein. This can be used to simulate the

protein in a computer. Using this model a three dimensional tour in the protein structure, exploring the confirmation of the protein, is possible. Another option is to highlight the main chain, the secondary structure or the different amino acids in a specific color. X-ray diffraction uses constructive interference to obtain data about the position of individual atoms in the molecule. For more information about x-ray diffraction see Appendix B .

Fluorescence Spectroscopy

This technique utilizes the fluorescence properties of certain molecules to gain information about the location of the fluorophores. The fluorophores can be excited at certain wavelengths and the returning emission light makes it possible to describe the placement of the fluorophore. This interplay is often used in thermal analyzes of macromolecules such as proteins. More information about fluorescence can be found in Appendix E .

Circular Dichroism

Circular Dichroism uses left and right circularly polarized light to analyze the secondary structure of a protein. This is possible because left and right circularly polarized light is absorbed differently in various molecular arrangements. The technique of Circular Dichroism is described in Appendix F .

1.5 How can proteins be related to nanotechnology?

As the size of proteins is generally between 4 and 50 nm and with the definition of nanotechnology in Section 1.3 we conclusively must accept proteins as nanostructures. Furthermore proteins can, in many contexts, be seen as nanomachines. For example the proteins aktin and myosin, found in muscle fibers, have the ability to contract and expand which enables humans or animals to move. [Poole and Owens, 2003]

1.6 Proteins

Introduction

The designation "protein" comes from the Greek word *proteios* meaning "primary" or "holding first place" [Britannica, 2004]. They are present and fundamental in every organism. Proteins are the most common macromolecules found in cells.

Cells can be described as a house, where proteins are the fixtures, furniture and most other part of the inside. Proteins are almost everything in the cell.

Some proteins help in digestion, others help in muscles with movement of the body and some constitute the main part of structures such as hair and nails. Yet

other proteins act as transport molecules. For instance the protein haemoglobin carries oxygen from the lungs to the rest of the body.

Structure

The basic structure of a native protein consists of up to 20 different amino acids, called α-amino acids. There are more than 100 amino acids in nature but only 20 of them occur in proteins. A combination of these amino acids bonded together in a chain is called a peptide. When 10 or more of these peptides are attached together it is called a polypeptide chain. If the chain is made of less than 10 amino acids it is often called oligopeptides. [www.oxfordreference.com1, 2004]

The backbone of the protein is the polypeptide chain and it often contains more than hundred amino acids. This way there are almost infinite possibilities to combine the 20 amino acids in a polypeptide. The backbone is often twisted in order to compact the protein as much as possible. To identify a protein it is necessary to look at the sequence of the amino acids in the polypeptide chain. Therefore it is essential to understand the structure of the amino acids, as these are the building blocks of the protein. [Encarta, 2003]

Amino Acid

The common structure of an amino acid consists of a central alpha-carbon (C) bonded to a hydrogen (H) atom, an amino group (H_3N), a carboxyl group (COO^-) and a side chain. Amino acids with side chains are referred to as amino acid residues. These side chains can be split into two classes, called the non-polar side chain and the polar side chain. The non-polar side chain mainly consists of hydrocarbon. They are incapable of participating in hydrogen bonding, instead they attract each other. Polar side chains contain groups that are able to participate in hydrogen bonding. [Britannica, 2004]

The size of amino acids varies from 0.42 nm (glycine) to 0.62 nm (tryptophan) in diameter, and the size of a protein is usually between 4 and 50 nm, as mentioned earlier. [Poole and Owens, 2003]

Figure 1.1 shows the structure of the 20 amino acid residues found in proteins. 19 out of the 20 residues all have the same common structure where the side chain is bonded to the carbon atom. The only difference is the structure of the side chain (marked with blue). The differences between these 19 residues and proline are that the amino group on proline is HN instead of the common H_3N and the side chain of proline is bonded to both the nitrogen and α-carbon atom. This is also showed on Figure 1.1 . All except glycine is considered asymmetric amino acids. Glycine is the smallest and simplest amino acid and it is symmetric because of the side chain that consists of a hydrogen atom [Creighton, 1993].

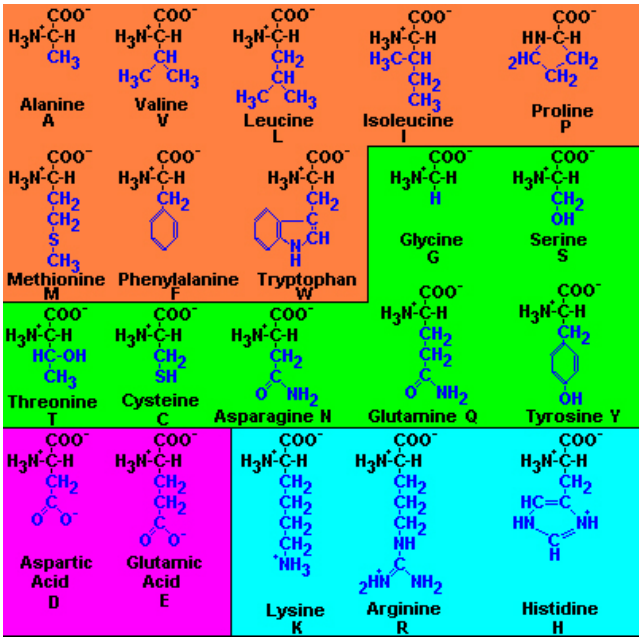

Figure 1.1: *The orange area indicates the 8 non-polar amino acids. The others are all polar. The amino acids in the pink area are acidic. The blue area is the alkaline amino acids. If in an alkaline solution the amino acid will have an* NH_3^+ *group and an COOH while in an acidic solution the groups will be of the form* NH_2 *and* COO^-*. [www.people.virginia.edu, 2003]*

Structure levels

For analysis purposes the proteins are broken down in four levels of structure. This makes it easier to identify the different characteristics of the protein. These levels are defined as follows by a committee of the International Union of Biochemistry. [Britannica, 2004]

Primary structure is the linear sequence of the amino acids in the peptide chain. Secondary structure shows the spatial structure of the backbone. Although the information about the arrangement of sidechains is in the primary structure, it determines the possibilities of secondary structure. The backbone is often coiled locally into helical regions and sheets, called α-helix and β-sheets, to become more compact. These are both stabilized and held together by hydrogen bonds. α-helix and β-sheets are the most important parts of the secondary structure. Other parts of the secundary structure is know as random coil. [Branden and Tooze, 2003]

Tertiary structure is determined by the interactions between the side chains of the amino acids. As the secondary structure illustrates information about the local folding, this structure is determined by folding of the whole polypeptide to make the protein more compact. In this level of structure it is possible to identify the disulphide bridges and the salt bridges. Covalent and ionic bonds are responsible for the shape

of both disulphide and salt bridges. The disulphide bridge is determined by the bond between the thiol groups of two cystine residues. [www.oxfordreference.com2, 2004]

A salt bridge is partly determined by the link between an acidic and basic group. It can be broken by a change in pH value and salt concentration. The salt bridges are important in connection with the structure of the protein and if the salt bridge is broken the protein is destabilised [www.oxfordreference.com3, 2004]. The acidic and alkaline groups are shown on Figure 1.1 . In Figure 1.3 a variety of bonds in the secondary and tertiary structure is displayed. In order to achieve a higher level of functionality multiple polypeptide chains can be combined into a protein. This is the quaternary structure [Mathews, 1995].

Types

Proteins can be divided into two groups; fibrous and globular. The main function of fibrous proteins is protection, such as the proteins in nails and hair. The polypeptide chain is arranged into long strings or sheets.

Globular proteins are folded into round or spherical shapes. These proteins works for instance as antibodies, certain hormones and enzymes.
[www.oxfordreference.com4, 2004]

1.7 Enzymes

Enzymes are proteins with the ability to catalyze a chemical reaction and they are therefore called natural catalysts. This catalytic effect has been used by man for several millenia without understanding the chemistry that lie beneath.

The modern history of enzymes dates back to 1833, where the French chemists Anselme Payen and Jean-Franois Persoz isolated an amylase complex from germinating barley and named it diastase. Two years later the Swedish scientist Jöns Jakob Berzelius described how amylase catalyzed the decomposition process of starch. The nature of enzymes remained hidden until 1926 were Dr. James B. Summer demonstrated that enzymes are proteins. He also performed the first crystallization of an enzyme. Crystallization is still an important technique that enables scientists to understand the structure of molecules with techniques such as X-ray diffraction, atomic force microscopy and optical microscopy [Novozymes, 2004]. From the mentioned techniques scientists has obtained a visual understanding of the protein structure. The introduction of supercomputers, with the capacity to calculate enormous amount of data within acceptable time, has resulted in methods of visualizing the protein structure, which has further increased the understanding of protein structures.

The increased knowledge of enzymes has led to a more specific use in the industry, which has resulted in new production methods and products. As examples of the use of enzymatic processes in industrial productions there are the products insulin, cheese, beer, more efficient washing powder and toothpaste.

Enzyme catalysis

To describe how the enzymes catalyze a reaction they have been classified into 6 key groups. These are described in Table 1.1 .

To catalyze a reaction an enzyme reacts with a substrate. The enzyme binds to the substrate on the surface. This place is called the active site of the enzyme and is formed as a pocket or channel. On large molecules the substrate can bind to more than one place. Furthermore the active site only allows one type of substrate to bind and the polypeptide in three dimensional arrangement determines the properties of the active site and therefore which substrate is allowed to be bonded. [Britannica, 2004]

Key group	**Function**
Oxidoreductases	Involved in the transfer of hydrogen or electrons between molecules
Transferases	Catalyze the transfer of a group of atoms from one molecule to another
Hydrolases	Catalyze the break down of a substance by adding or removing water
Lyases	Catalyze either the cleavage of a double bond and the addition of new groups to a substrate, or the formation of a double bond
Isomerases	Catalyze the rearrangement of the atoms within a molecule
Ligases	Catalyze the formation of covalent bonds using the energy released by the cleavage of an energy-rich phosphate bond

Table 1.1: *The 6 key groups briefly describes how enzymes catalyses a reaction [www.oxfordreference.com5, 2004]*

1.8 Lysozyme

An example of a common enzyme is lysozyme. It was discovered by Sir Alexander Fleming in 1921, when a drop of his nose secretion fell into a dish of different bacteria. As an area of the bacteria in the dish was destroyed, Sir Alexander Fleming studied the effect and found the enzyme lysozyme.

The function of lysozyme is to catalyze the break down of the cell wall of certain bacteria by catalyzing the insertion of a water molecule between a C-O bond and therefore belongs in the hydrolases key-group. Lysozyme is found in most living organisms such as egg white, tears, salvia and breast milk. Hen egg white lysozyme is

one of the most studied enzymes and consists of 129 amino acid residues. Its structure is similar to ones commonly found in globular proteins [www.rostra.dk, 2003]. A more detailed explanation and illustration of lysozyme can be found in Section 3.4 .

1.9 Quantum States

As described earlier the best way of describing structures on the nano scale, such as enzymes and proteins, is quantum mechanics. Electrons in an atom, orbit the nucleus in predefined states called quantum states. These quantum states are specified by four quantum numbers called the principal orbital number, the orbital quantum number, the orbital magnetic quantum number and the spin magnetic quantum number. The quantum numbers describe the probability of finding the electron within a volume called the orbital. The electron is described when these four quantum numbers are known. [Serway and Beichner, 2000]

The Principal Orbital Number

The principal orbital number describes the energy level and nucleus separation of the electron, and it is denoted by n. It is sometimes said to denote the shell in which the electron is orbiting. The energy level of the electron is directly related to n. While n increases the distance between the electron and the nucleus, and thereby the energy, increases too. This relation is described by Equation 1.1 . [Serway and Beichner, 2000]

$$E_{n,l,m_1} = \frac{-13.6eV}{n^2} \tag{1.1}$$

The energy level of a free electron is defined to be zero. A free electron corresponds to n approaching infinity, which makes E approach zero. With $n = 1$ the electron has the energy $-13.6eV$ which is the lowest possible energy of an electron. The higher the energy of the electron, the lower energy is needed to ionize the atom. [Serway and Beichner, 2000]

The other Quantum Numbers

The orbital quantum number divides the shells described by the principal orbital number into subdivisions and it is denoted by l. It is related to the angular momentum, by the relation in Equation 1.2 .

$$L = \sqrt{l(l+1)}\hbar \tag{1.2}$$

Where L is the angular momentum and $\hbar$ is plancks constans divided by 2π. The orbital quantum number is an integral number $l = 0, 1, 2 \ldots n-1$. The numbers are often denoted with characters $s, p, d, f \ldots etc$, where s corresponds to $l = 0$. Furthermore, as stated earlier, there are the orbital magnetic quantum number m_l,

and the spin quantum number m_s. The magnetic quantum number is in the range $-l, -l-1 \ldots -1, 0, 1 \ldots l-1, l$ and the spin quantum number can be either 1/2 or $-1/2$, or spin up and spin down respectively. According to Pauli Exclusion Principle no more than one electron is allowed to occupy the same four quantum numbers at the same time. This is due to the fact that electron favor the principle of lowest possible energy. If two electrons are having the same four quantum numbers, they are within the same orbital and therefore repel each other to a larger extent than if they were in two different orbitals. [Serway and Beichner, 2000]

1.10 Molecular bonds

In a molecule both repulsive and attractive inter atomic interactions are found. Both the repulsive and the attractive forces are strongly dependent on the separation distance. The attractive force is a result of the attractive part of the coulomb interaction, the gravity being of no importance on this scale, which is increasing inversely proportional to the distance. The repulsive force is a combination of the repulsive part of the coulomb interaction and at small distances overlapping of electron orbital with respect to Pauli Exclusion Principle. In the repulsive coulomb interaction occurs mainly between the electrons of the two atoms and to a smaller degree between the two nucleus. The resulting force as a function of the separating distance is shown in Figure 1.2 .

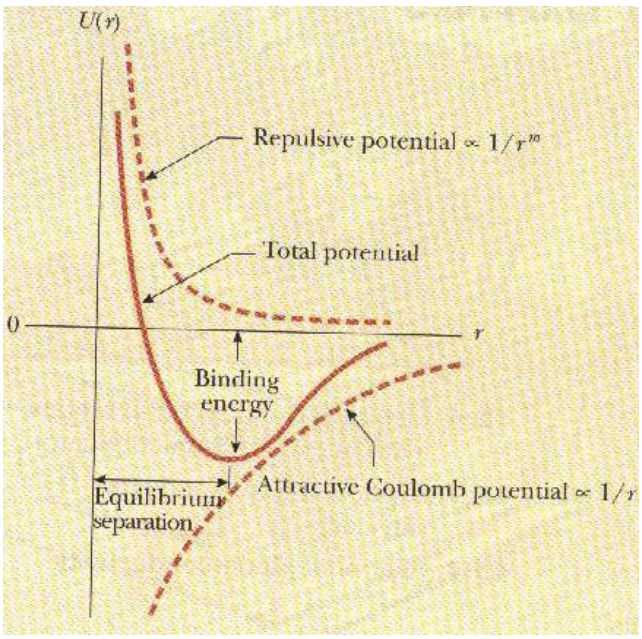

Figure 1.2: *The resulting system energy as a function of the internuclear distance [Drenth, 2002].*

In order for atoms to arrange in a molecule the energy of the molecule must be less than the sum of energies from the single atoms. The total description of the binding forces in a larger molecule is complex due to the amount of atoms and thereby interactions in the molecule. The description is simplified into four different models: Ionic, covalent, van der Waal and hydrogen bonding.

The ionic bond is characterized by almost total displacement of the binding electron orbitals. The most common example of this binding is kitchen salt, $NaCl$. The $3s$ electron of sodium is displaced towards the chloride in order to fill its outer shell forming the electronic structure of argon. The energy gained by forming this binding is equal to the difference between the cost of ionizing the two atoms and the energy gained by connecting the two atoms in the internuclear bond.

In a covalent bond the outer electron orbits are dislocated due to electrostatic forces. The electron orbitals can no longer be described as belonging to their respective atom but the description must be for the entire system. New shared orbitals are formed. It may be described from the example of two hydrogen atoms in a covalent bond. The electron of the hydrogen atom can exist in two different quantum states, the magnetic spin up or down. Due to Pauli exclusion principle a covalent bond between the two hydrogen atoms can only exist when the electrons exist in different spin quantum states. This is called the binding orbital whereas two similar spin quantum states would displace one electron in a higher quantum state resulting in an anti binding orbital. The force of the bond is a result of a positive overlap in the outer electron orbital of the atoms involved. In the binding orbital there are a probability of finding the electron between the two hydrogen nucleus bound via the coulomb force. [Serway and Beichner, 2000]

These two type of bonds are the strongest internucleus bonds. Both of these are in the eV magnitude. Two common bonds like the NaCl ionic bond and the C-C bond have an energy of respectively 4.2 eV and 3.6 eV. [Andersen et al., 1986]

Between two separated molecules a weak attractive force exist, and the same force exist between two atoms not connected trough a covalent or ionic bond. This attraction force is due to an electric dipole moment. There are three types of van der Waal forces. The strongest is the dipole-dipole, based on the attraction between two permanently dipolar molecules. A dipolar molecule can induce a dipole moment in a nonpolar molecule creating a weak van der Waal bond compared to the permanent dipole. In nonpolar molecules the electron charge distribution is uneven and a weak self induced dipole can occur. When this self induced dipole induce a dipole in a surrounding molecule it results in an attracting force. This kind of van der Waal bond is found in gasses like H_2, O_2 or in inert gasses. [Serway and Beichner, 2000]

In a H_2O molecule there are a permanently dipole. The atoms oxygen and hydrogen are respectively charged positive and negative. This results in a van der Waal attraction but the interaction between the oxygen and hydrogen atoms are considerably stronger. The relatively high level of surface tension in water is due to this type of bonding. There are hydrogen bonds in many contexts and they are partly responsible for the spatial structure of proteins and for the double helix of DNA. The strength of a hydrogen bond is around 5% of a typical covalent bond. In

a protein all the above mentioned bonds exist. [Serway and Beichner, 2000]

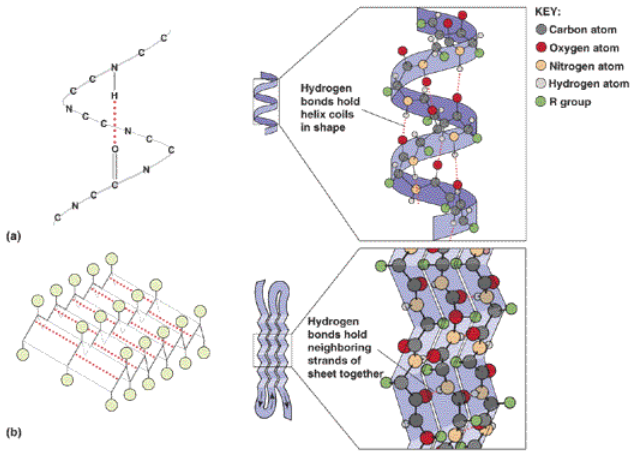

Figure 1.3: *The hydrogen bonds of the secondary structure is shown. [Britannica, 2004]*

Molecular bonds in a crystal

Atoms and molecules in the solid state is either arranged in a crystalline pattern or in an amorphous state. In the process of forming the solid it will seek the lowest level of energy. One way of releasing a high amount of energy is by an arrangement in a crystalline pattern. The covalent and ionic bond are appropriate for description of bonds in solids. [Serway and Beichner, 2000]

1.11 Crystalline structure

A crystal is matter in the solid state where the atoms are ordered in a periodic arrangement. Ideally, it is an infinite repetition of identical atoms or of a structure of atoms. In Figure 1.4 the definition of a crystal is described. The crystal can be described as if the bases where attached to points in a lattice.

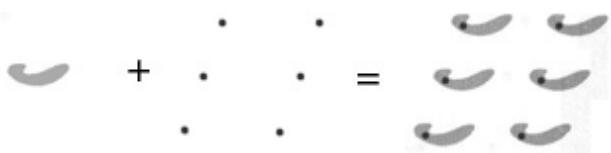

Figure 1.4: *The basis is added to the lattice forming the crystal. Note that the lattice is a net in three dimensions, while only two dimensions are displayed here. Basis + Lattice = Crystal. Modified from [Kittel, 1996]*

It does not matter if the lattice is displaced as long as it fulfils the criteria of the lattice definition. The points of the lattice are defined by the addition of the translation vector to one point of the lattice:

$$R1 = R + \mathbf{T}, \mathbf{T} = n1\mathbf{a1} + n2\mathbf{a2} + n3\mathbf{a3} \tag{1.3}$$

a1, **a2** and **a3** being the unit vectors of the lattice and $n1$, $n2$ and $n3$ being arbitrary integers. The translation vector, **T**, describes the difference between the two points, R and $R1$. The relation between two points, when suitable numbers, $n1$, $n2$ and $n3$ are chosen, can be described by the translation vector, the lattice and the basis are primitive. This means that the lattice units are the smallest possible. Several lattices may be chosen for one crystal. For either choice the same results of analyses including x-ray diffraction pattern ensue as long as the translation vector of Equation 1.3 has been satisfied. The crystal can be defined with basis in the growth of bases on top of each other or from a given lattice as long as Equation 1.3 is maintained. This will have no effect on results. In a lattice it is possible to chose several different unit cells, however, a distinction between the primitive unit cell and the unit cell is necessary. The primitive unit cell is defined as minimum volume cells. Each primitive cell has only one lattice point attached and for a given crystal the number of atoms in the primitive cell is invariable. A normal choice of primitive cell is the parallelepiped. In Figure 1.5 different primitives cells, cell 1, 2 and 3 and one nonprimitive cell 4, are shown. [Kittel, 1996]

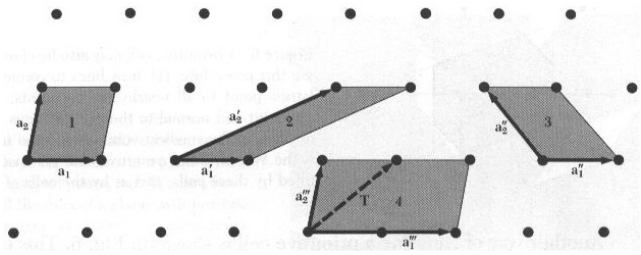

Figure 1.5: *The choice of different unit cells is possible. 1,2 and 3 are primitive cells while 4 is not.*

For a parallelepiped primitive cell, see Figure 1.6 , the number of lattice points touched by the primitive cell is 8, and when neighbouring 8 identical cells the number of associated lattice points must be: $8 \cdot 1/8 = 1$. The volume of this parallelepiped cell is determined by:

$$V = |\mathbf{a1} \cdot \mathbf{a2} \times \mathbf{a3}| \tag{1.4}$$

There are fourteen different lattice types characterized by angles and side lengths. Triclinic is the general lattice with no identical angles or sides [Kittel, 1996]

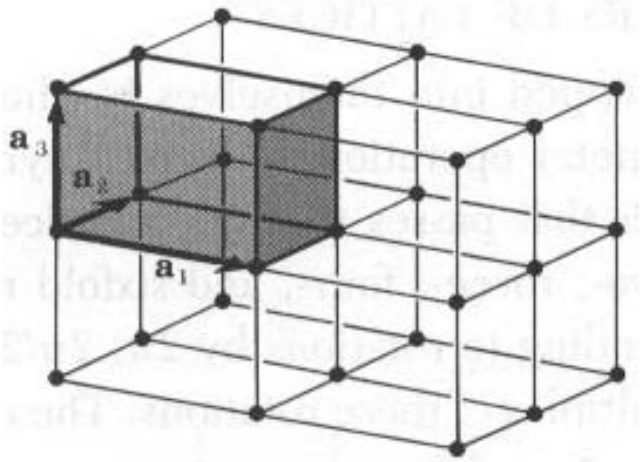

Figure 1.6: *The cell determined by the vectors a1,a2,a3 is a primitive parallelepiped unit cell [Kittel, 1996].*

Planes in crystals

Crystal planes can be described by three points in the plane provided that they are not collinear. If the points lie on each of their crystal axis the points can be described by the lattice constants, **a1**, **a2** and **a3**. The miller index, *(hkl)*, is associated with the plane and it is advantageous to describe the plane through this index. It is the smallest vector of integers and is determined by the following equation, where c is the number needed for h, k and l to be the smallest integers possible:

$$(hkl) = c \cdot \left(\frac{1}{a1}, \frac{1}{a2}, \frac{1}{a3}\right), (h, k, l) \in N \tag{1.5}$$

For the crystal points $(2, 4, 1)$ the index is:

$$(hkl) = c \cdot \left(\frac{1}{2}, \frac{1}{4}, \frac{1}{1}\right) \Rightarrow c = 4 \Rightarrow (hkl) = (214) \tag{1.6}$$

For a given macro crystal the lattice type is not always easily identified. The visible structure sometimes gives a hint about the lattice type, for example cubic crystal structure tend to form rectangular crystals. The surface of a crystal is a crystal plane and it is possible to name the surface using the miller index. The angles of the macro crystal can help identify the lattice. For example oblique angles indicate a triclinic crystal structure. [Serway and Beichner, 2000]

1.12 Project limitations

The approach to this project is "Structures and conditions". The subject leads us back to the initiating problem: "How can different techniques be used to examine

molecule structures and to determine the properties of these structures“. To answer the question it is necessary to look into which different techniques exist, how molecules are built and ultimately try some of the techniques ourselves. An angle of approach to the subject is to examine a specific enzyme using the techniques. In this project the enzyme lysozyme is examined. Lysozyme is a very accessible enzyme; furthermore it is a closely studied enzyme. In order to collect data about the enzyme structure a series of experiments has been planed. The experiments will include protein crystallization and analysis of the protein crystal structure through optical microscopy. Moreover computer simulations of the spatial structure of lysozyme will be studied. Lysozyme will be studied using fluorescence spectroscopy and circular dichroism. In order to work with the AFM it is necessary to use a more stable crystal than protein crystals, therefore $CuSO_4$ has been chosen. Lastly absorbance spectroscopy of $CuSO_4$ has been planned.

In connection with the experiments we will discuss the collected data. We have decided to use the described techniques, but there are other ways of studying proteins for instance, dynamic light scattering, X-ray diffraction and differential scanning calorimetry. Due to the time frame it is decided not to use these methods.

1.13 Problem statement

The purpose of this project is to gain knowledge in the field of structure analysis, to learn different techniques, to evaluate the outcome of the analyses and to gain knowledge in the field of nanotechnology. Our angle of approach to the subject is through $CuSO_4$ and the enzyme lysozyme.

The focus of the report will be the techniques listed in ”Project limitations“. In this context the following questions are relevant:

- How do we interpret the various data and do the different data supply each other?
- What does the data tell us and how do we translate data to a model of reality?
- Do these models represent reality?

Chapter 2

Methods

2.1 Procedure of Experiments

This section serves the purpose of describing how the experiments were conducted and which materials were used.

2.2 Crystal growth

In order to use atomic force microscopy or X-ray diffraction, a single crystal of a certain size, for X-ray a few 0.1mm [Nolting, 2004], is needed. This is rarely a simple process and multiple attempts are needed to achieve suitable crystals. For more information about growing crystals see Appendix A .

$CuSO_4$ crystals can be achieved by placing a drop of a $CuSO_4$ solution on a microscope slide. The drop is brought to oversaturation by evaporation and crystals are formed.

Before the lysozyme crystallization experiment, the enzyme solution ($100mg/mL$) must be centrifuged at 10,000 rpm for 10 minuttes in order to remove any aggregated protein molecules. Using the sitting drop method, see Figure A.1 , a setup of 24 wells were made with varying pH, precipitant concentration and type. The two different precipitants used where kitchen salt, $NaCl$, and ammonium sulphate, $(NH_4)_2SO_2$. In Table 2.2 an overview of the parameters of the different wells are displayed. The different solutions are made using $4MNaCl$, a $5M(NH_4)_2SO_2$ solution and two buffers, sodium acetate and Tris/HCl to achieve a pH of 4.8 and 8.7 rescpectively. From each of the solutions 1mL is added to the exterior well. In the interior well 1μL from the precipitant solution and 1μL of lysozyme solution is added. When a series of 6 wells are filled they must be sealed with tape to prevent evaporation. After 24 hours the crystallization process is done. Pictures of the wells using optical microscopy are shown in Section 3.1 .

$$V_1 \cdot c_1 = V_2 \cdot c_2 \Leftrightarrow V_1 = \frac{V_2 \cdot c_2}{c_1} = \frac{1.4mL \cdot 0.7M}{4M} = 0.2625mL \tag{2.1}$$

		$NaCl$		$(NH_4)_2SO_2$	
		A (pH 4.8)	B (pH 8.7)	C (pH 4.8)	D (pH 8.7)
1	[c]	0.75M	0.75M	0.75M	0.75M
	V_{salt}	0.26mL	0.26mL	0.21mL	0.21mL
	V_{buffer}	1.14mL	1.14mL	1.19mL	1.19mL
2	[c]	1.00M	1.00M	1.00M	1.00M
	V_{salt}	0.35mL	0.35mL	0.28mL	0.28mL
	V_{buffer}	1.05mL	1.05mL	1.12mL	1.12mL
3	[c]	1.25M	1.25M	2.00M	2.00M
	V_{salt}	0.44mL	0.44mL	0.56mL	0.56mL
	V_{buffer}	0.96mL	0.96mL	0.84mL	0.84mL
4	[c]	1.50M	1.50M	3.00M	3.00M
	V_{salt}	0.53mL	0.53mL	0.84mL	0.84mL
	V_{buffer}	0.87mL	0.87mL	0.56mL	0.56mL
5	[c]	1.75M	1.75M	4.00M	4.00M
	V_{salt}	0.61mL	0.61mL	1.20mL	1.20mL
	V_{buffer}	0.87mL	0.87mL	0.56mL	0.56mL
6	[c]	2.00M	2.00M	5.00M	5.00M
	V_{salt}	0.70mL	0.70mL	1.40mL	1.40mL
	V_{buffer}	0.70mL	0.70mL	0mL	0mL

Table 2.1: *In order to reach the scheduled values of precipitant concentration, [c], an amount, V, of the original precipitant solution is added. From each of the solutions 1mL is added to the respective well.*

2.3 Optical Microscopy

The microscope is able to magnify an subject up to 2000 times, in this experiment a magnification factor 10 and 20 is used. Optical microscopy is a very useful tool to examine the shape of the materials. The microscope can be used on a sample placed on a transparent surface, and the material is thereby magnified. The microscope has its limits, but for preliminary examination it is a valuable tool, however a there is a lack of depth perception.

The crystals from the crystallization experiment is studied using this technique. With a camera extension pictures of the crystals are recorded. This enables a measurment of angles in the crystal. The angles are measured using the program SmartSketch™.

2.4 Atomic Force Microscopy

The atomic force microscope works by dragging a tip, mounted on a cantilever, over the sample and thereby measuring the topography. The position of the tip can be controlled with high precision so it is possible to examine regions in micro-

and nanometer scale, thus making it possible to examine crystals or small areas of a surface. The data is also used to determine the roughness (the scale for height variation) and angles in the crystals. See Appendix C for more information.

$CuSO_4$ is chosen for its ability to make rather large crystals in a short time. The crystals made from $CuSO_4$ were examined using atomic force microscopy and the typography, roughness and the angles on the crystals were measured.

RMS Roughness

One way of measuring the roughness of a surface, is to use the RMS roughness which can be computed using the formula in Equation 2.2 . [www.nanosurf.com, 2004]

$$r = \sqrt{\left(\sum_{x,y} \frac{\left(Z_{x,y} - \overline{Z_{x,y}}\right)^2}{n}\right)}, \quad \overline{Z_{x,y}} = \frac{1}{n} \cdot \sum Z_{x,y} \tag{2.2}$$

In this formula $\overline{Z_{x,y}}$ is the average height and the sum is calculated over all measured values.

Angles

The angles are measured using the Nanosurf$^{\mathbf{TM}}$ program. They are measured orthogonally to the edge of the crystals by making a crosssection and then using the angle measurement tool. [www.nanosurf.com, 2004]

2.5 Absorption Spectroscopy

Light is send through a solution of the substance to be examined, and the transmission is measured as a function of the wavelength of the light. The absorptions spectrum is calculated using Equation 2.3 . The amount of light absorbed at a given wavelength depends on the concentration of the solution, the chemical composition and the traveling distance of the light through the solution. This correlation is described by Beer-Lambert's law shown in Equation 2.3 .

$$I = I_0 \cdot 10^{-\epsilon c l} \tag{2.3}$$

The intensity I is measured when the light has traveled the distance l through the solution, I_0 is the input intensity, ϵ is the molar absorption, and c is the concentration of the solution. The absorbance A is defined in Equation 2.4 .

$$A = \log \frac{I_0}{I} = \epsilon c l \tag{2.4}$$

Absorption of light with at a given wavelength is caused by the various energy levels with the corresponding energy difference found in the solution. Thereby information about the energy levels is achieved. The software automatically calculates the absorption.

Two experiments with absorption spectroscopy included a solution of $CuSO_4(aq)$ and the same solution with NH_3. Firstly an absorption spectrum for clean water is made for reference. Then a solution of $CuSO_4$ is made with 130 mg $CuSO_4$ is dissolved in 3 mL H_2O. The absorption spectrum for the $CuSO_4$-solution is measured. Lastly 500 μL NH_3 (25% solution NH_3) and 3 mL H_2O is added and the absorption spectrum is recorded.

2.6 Visualization

By studying the structure file 1DPX, from the Protein Data Bank, it is possible to determine the different structures of the lysozyme found in hen egg white. The structure file is based on data from X-ray diffraction analysis at a resolution of 1.65 Å and contains spatial coordinates for the atoms of the proteins. Using these data it is possible to study the spatial structure of proteins in visualization software. [www.rcsb.org/pdb, 2004]

PyMOL, [pymol.sourceforge.net, 2004], is an open source graphic system designed for visualizing images and animations of molecules. The purpose of the visualization experiment is to locate the following structures:

- α-helices
- β-sheets
- Disulphide bridges
- Salt bridges
- Active site

2.7 Fluorescence Spectroscopy

Fluorescence spectroscopy is used to identify and localize the fluorophores of molecules utilizing emission properties of certain amino acid residues.

The cuvette was cleaned in 2% deconex, H_2O and 70% ethanol, and dried with compressed air. The slit size was set to $4nm$. For the solvent a 15 μM 3 mL lysozym solution without quencher were made. This solution was made from a 226 μM stock solution.

Glycin buffer from a $100mM$ stock solution was added to make the lysozym solution a $25mM$ glycin solution. The calculation is shown in Equation 2.5 .

$$c_1 \cdot V_1 = c_2 \cdot V_2 \Rightarrow 15\mu M \cdot 3000\mu L = 226\mu M \cdot V_2 \Rightarrow$$
$$V_2 = \frac{3000\mu L \cdot 15\mu M}{226\mu M} = 119.12\mu L \quad (2.5)$$

Four additional lysozym solutions were made and $CuCl_2$ were added as a quencher. The quencher was taken from a 10 mM stock solution. A 0.025, 0.05, 0.1 and 0.15 mM $CuCl_2$ solution was made. The calculation was made similar to Equation 2.5 .

Table 2.1 shows the amount of each stock solution that must be mixed with demineralized water in order to reach the correct concentration.

Stock/Final	$226\mu M$ Lys.	$100mM$ Gly.	$10mM$ $CuCl_2$	Water
Buffer	–	$750\mu L$	–	$2250.00\mu L$
Lysozyme	$199.12\mu L$	$750\mu L$	–	$2050.88\mu L$
$0.025mMCuCl_2$	$199.12\mu L$	$750\mu L$	$7.5\mu L$	$2043.38\mu L$
$0.050mMCuCl_2$	$199.12\mu L$	$750\mu L$	$15\mu L$	$2035.88\mu L$
$0.100mMCuCl_2$	$199.12\mu L$	$750\mu L$	$30\mu L$	$2020.88\mu L$
$0.150mMCuCl_2$	$199.12\mu L$	$750\mu L$	$45\mu L$	$2005.88\mu L$

Figure 2.1: *The table shows the solutions used in the fluorescence experiments, and how much of each stock solution was used to mix the solution.*

An emission spectrum between 300 and $450nm$ with excitation at $288nm$ was measured on each of the six solutions shown in the table. A temperature spectrum of the enzyme solution without $CuCl_2$ from $20 - 85°C$ is measured. The speed of temperature increase is set to $1.5°C$ per minute and the monitor wavelength is 350 nm. A spectrum before and after heating is made. See Appendix E for the theory behind Fluorescence Spectroscopy.

Stern Volmer constant

The ratio of the fluorescence intensity with and without a quencher is descibed by the Stern Volmer equation as seen in Equation 2.6 . For more information about quenching see Appendix E .

$$\frac{F_0}{F} = 1 + k_q \tau_0 \cdot [Q] \tag{2.6}$$

A plot of the ratios will be located on a line of the form $y = a + bx$ according to the Stern Volmer theorem. The y values are the relationship between the intensity of the fluorescence before and after the quencher was added. a equals 1 and b is the constant $k_q\tau_0$. If y_i equals $\frac{F_0}{F}$ and x_i equals $[CuCl_2]$ then the a and b values can be computed using Equation 2.7 .

$$b = \frac{\sum(y_i - \overline{y})(x_i - \overline{x})}{\sum(x_i - \overline{x})^2} \tag{2.7}$$

where $\overline{x} = \frac{1}{n}\sum x_i$, $\overline{y} = \frac{1}{n}\sum y_i$ and $a = \overline{y} - b\overline{x}$.

2.8 Circular Dichroism

Circular dichroism was used to estimate the distribution of secondary structure using the characteristics of chiral molecules in absorption of circularly polarized light.

The cuvette is cleaned in H_2O and buffer and dried using compressed air. A 500 μL enzyme solution consisting of 15 μM lysozyme and 25 mM glycin is made from a 226 μM lysozyme stock solution, and a 100 mM glycin stock solution. While increasing the temperature from 20 to 90°C the absorption at 220 nm is recorded. The temperature ramp is set to 1.5°C per minute.

The experiment is conducted three times. The average value of the three experiments are calculated by the software to make a graph that compensates for deviation in the single data. The buffer used in the experiment is glycine at pH 10. Before analyzing the protein a spectrum of the buffer is made. This spectrum is used as a reference value to eliminate the absorbance of the buffer. After the buffer spectrum has been recorded a spectrum of the lysozyme solution is made. Both of these spectrums are recorded to determine the wavelength at which the absorption is at maximum. This specific wavelength is used to measure the absorption with respect to temperature.

When the analysis of lysozyme is prepared, the cuvette is closed with a stopper to prevent evaporation from the cuvette while it is heated. If evaporation were allowed it would make the concentration of protein higher as the liquid escaped from the cuvette and therby making the data invalid. A high concentration of protein in the cuvette would prevent light from getting to the detector causing interference in the data.

The heating experiment is made with a linear temperature curve. The temperature rise is 1.5°C pr. minute starting at 20°C.

Distribution of secondary structure

The program k2d, [www.embl heidelberg.de, 2004], is used to estimate the distribution of the secondary structure. The program compares a set of circular dichroism spectra ranging from 200 nm to 241 nm with 16900 known values from other proteins. This program uses $[\theta]_{MRW}$ (Mean Residue Weight ellipticity) and therefore it is necessary to convert the output data from the experiment to this unit. Equation 2.8 can be used for this conversion.

$$[\theta]_{MRW} = \frac{\theta}{10^{-4} \cdot c \cdot l \cdot n} \left[deg \cdot cm^2 \cdot dmol^-1\right] \tag{2.8}$$

In the equation θ is the ellipticity, c is the concentration, l is the path length and n is the number of amino acids. See Appendix F for the theory behind circular dichroism.

Chapter 3

Results

3.1 Optical Microscopy

Lysozyme

The pictures in Figure 3.2 shows microscope magnifications of lysozyme crystals in 20x magnification. These crystals are from well number C_5 and C_4, which utilized $(NH_4)_2SO_4$ as precipitant at a concentration of $4M$ and $3M$, respectively, at pH 4.8. The left picture in Figure 3.3 is from well C_1 under the conditions $0.75M(NH_4)_2SO_4$ at pH 4.8. Multiple crystals have grown together making them unsuitable for X-ray diffraction. Furthermore crystals in well B1 were achieved although they appear different under the conditions, $0.75MNaCl$ pH 8.7. This may be due to a different crystal structure or it could be crystallized $NaCl$, see the right picture in Figure 3.3 .

Copper sulphate

The pictures in Figure 3.1 shows microscope magnifications of $CuSO_4$ crystals at 10x magnification. The obtuse angles of the crystals are measured using Smart sketch and found to be 123° in average. The measured angles is listed in Table 3.1 .

Picture number	**Degrees measured**
$CuSO_4$ 3	122.7°
$CuSO_4$ 4	122.8°
$CuSO_4$ 7	122.8°
$CuSO_4$ 8	121.7°
$CuSO_4$ 9	125.2°

Table 3.1: *The angles measured from the respective microscope pictures. The referenced pictures can be found on the attached CD.*

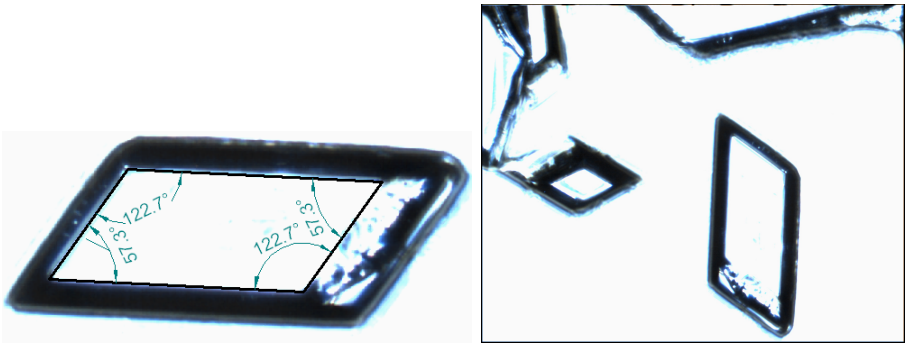

Figure 3.1: *An image of a $CuSO_4$ crystal using a magnification factor of 10. The crystal was grown drying a drop of $CuSO_4$ solution on a microscope slide. This picture is $CuSO_4$ 3.*

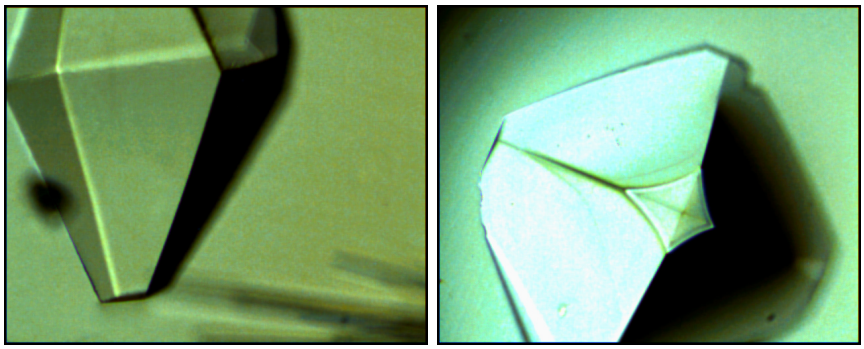

Figure 3.2: *Crystallized lysozyme. The pictures are respectively from the wells c5, $4M(NH_4)_2SO_4$, and c4, $3M(NH_4)_2SO_4$, both at pH 4.8. Both the crystals are large single crystals suitable for X-ray diffraction. See Section 2.2 for information about the crystal growth experiment setup. [A306, 2004]*

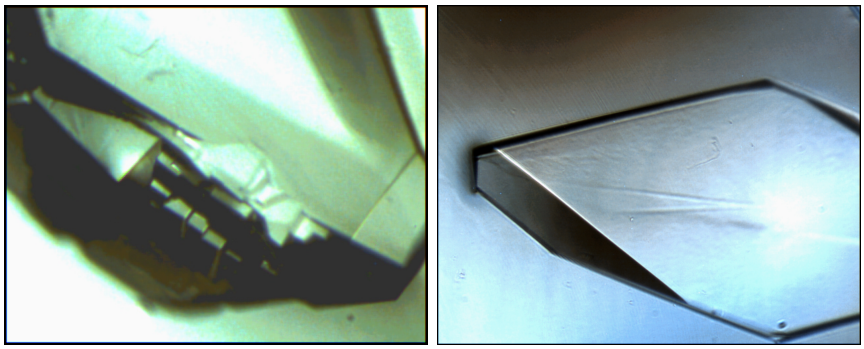

Figure 3.3: *To the left, from well c1, $0.75M(NH_4)_2SO_4$ at pH 4.8, multiple crystals have grown on top of each other making the crystal useless for X-ray diffration. The right picture is from well b1, $0.75MNaCl$ pH 8.7, and appear to have a different crystal structure. [A306, 2004]*

3.2 Atomic Force Microscopy

Figure 3.4 shows the topography of a $CuSO_4$ crystal made using an atomic force microscope. The left part of the picture shows a cross sectional view of the topography, and the right part shows a top view of the topography. These pictures have been used to calculate the roughness and measure the angles of the crystals.

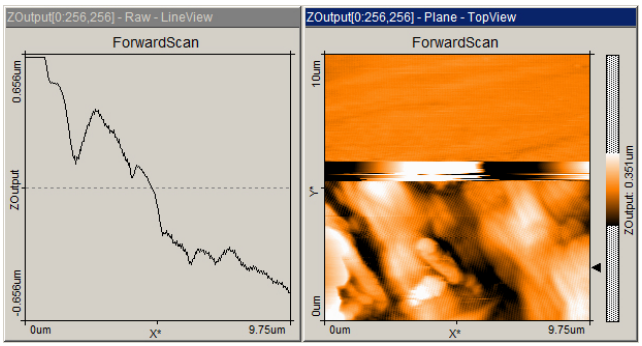

Figure 3.4: *The topopgraphy of an $CuSO_4$ crystal measured using the AFM instrument. The experiment was stopped due to some sudden vibrations. The area scanned is a square with sidelength 10 μm. To the left the cross sectional view is shown. The corresponding point is denoted in the right image by the black triangle.*

Calculation of roughness

The roughness of the surface examined by atomic force microscopy is calculated using the RMS roughness formula presented in Section 2.4 .

In Table 3.2 the roughness of the scans are shown. They are calculated using Equation 2.2 . The roughness is measured in μm.

Scan number	**Roughness** μm
1	0.096
2	0.105
3	0.116
4	0.125

Table 3.2: *The table shows the calculated roughness values. Scan 4 is from [A306, 2004]. The calculations and images can be found on the attached CD.*

Measurement of angles

Different angles are measured as described in Section 2.4 . The results of these measurements are taken from scan1. The angles were measured at an average of 132°. The scans can be found on the attached CD.

3.3 Absorbance Spectroscopy

Figure 3.5 through Figure 3.8 show absorbance and transmission spectrums of 0.17 M $CuSO_4$, and 0.17 M $CuSO_4$ added $500\mu L$ NH_3. The images show the absorbance spectrums of the solutions.

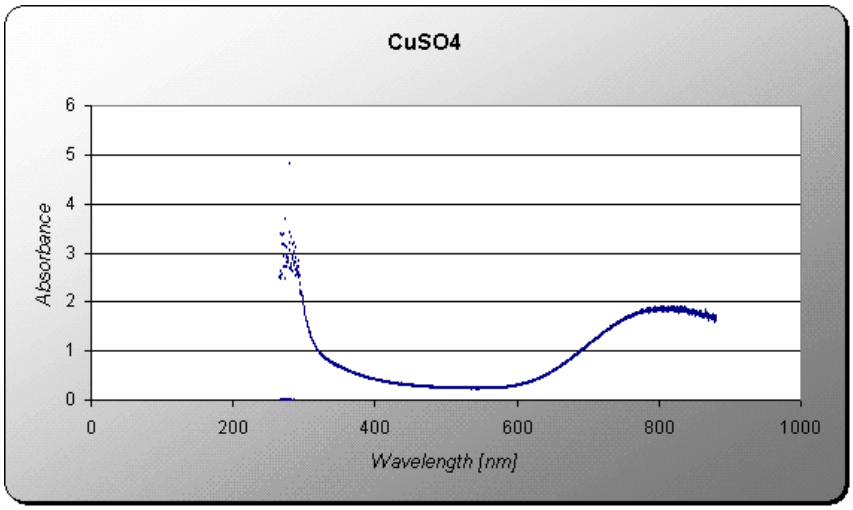

Figure 3.5: *The absorbance of light in a solution of 0.17M $CuSO_4$ is presented. As it can be seen in the image, the solution does not absorb light between 350 and 600 nm. It absorbs strongly below 350 and above 700nm.*

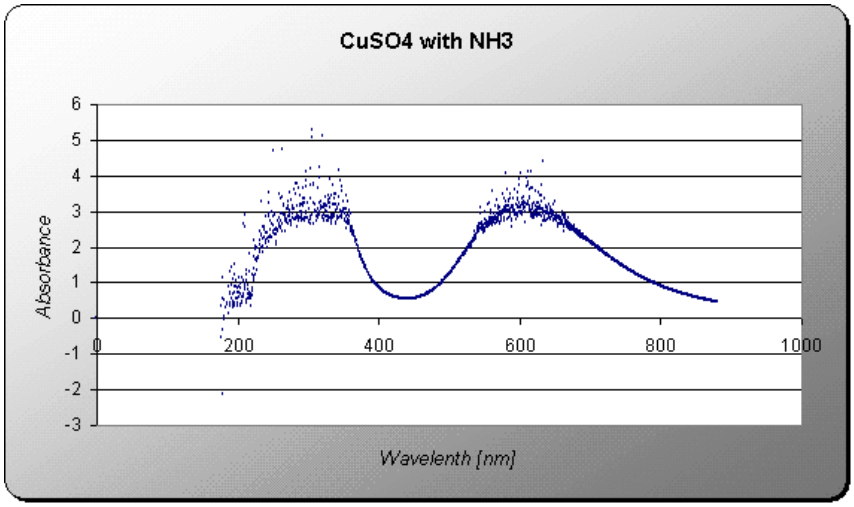

Figure 3.6: *The absorbance of light in a solution of 0.17M $CuSO_4$ added 500 μL NH_3 is shown. The solution absorbs light below 350 nm and above 550 nm. Between 350 nm and 550 nm the light can pass through the solution.*

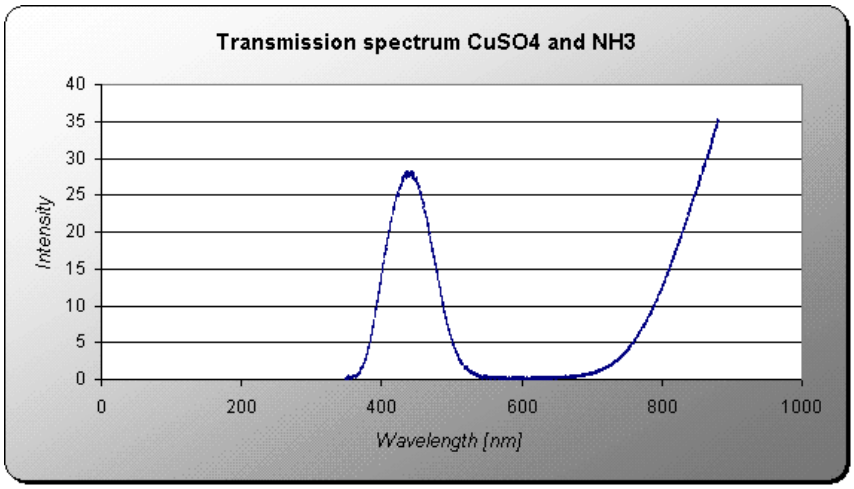

Figure 3.7: *The transmission light through the 0.17M $CuSO_4$ with 500 μL NH_3 solution is shown. Light between 350-550 nm passes through the solution, which is light in the blue area. Nor is light absorbed above 700nm, which is in the infrared area.*

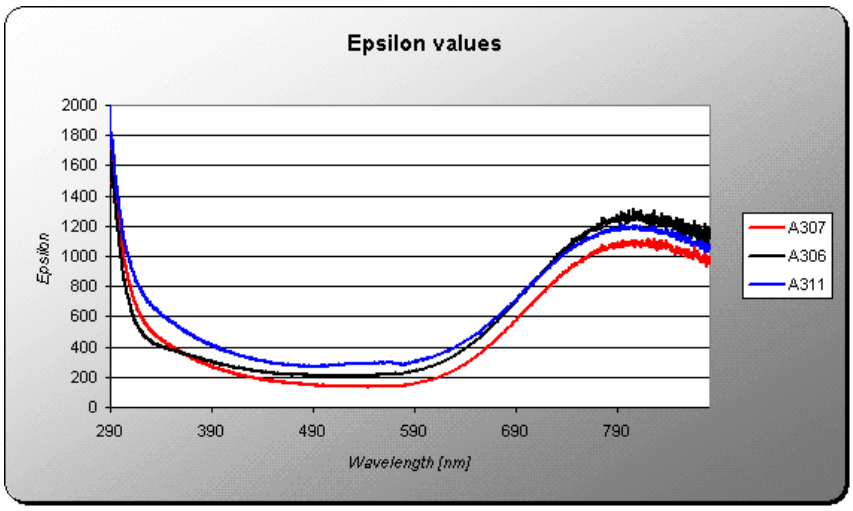

Figure 3.8: *In this figure the epsilon values from the three different experiments are shown. The $CuSO_4$ concentrations used are 0.133M, 0.17M and 0.16 for A311, A307 and A306 respectively. [A306, 2004] [A311, 2004]*

3.4 Visualization

As described in Section 2.6 the characteristics of the enzyme lysozyme has been found and emphasized. In Figure 3.9 the secondary structure is displayed, Figure 3.10 and Figure 3.11 illustrates the tertiary structure. In Figure 3.12 the location of tryptophan amino acid residues which will be futher commented in Section 4.4

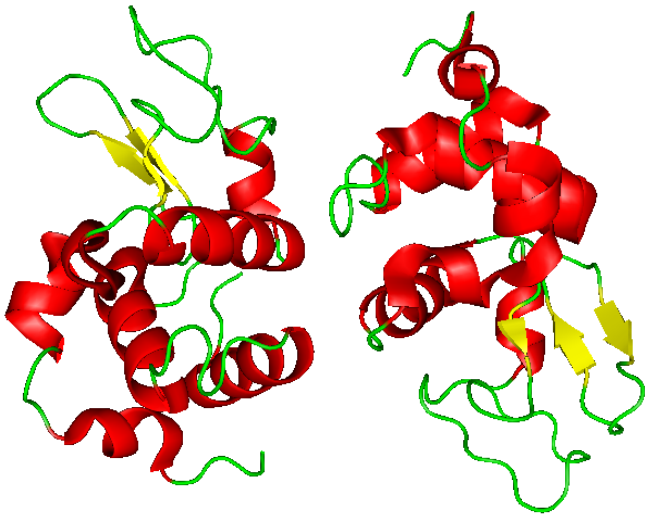

Figure 3.9: *In lysozyme there are 7 α-helices marked with red and 3 anti-parallel β-sheets marked with yellow. The remaining green string is the random coil. These constitutes the secondary structure of lysozyme.*

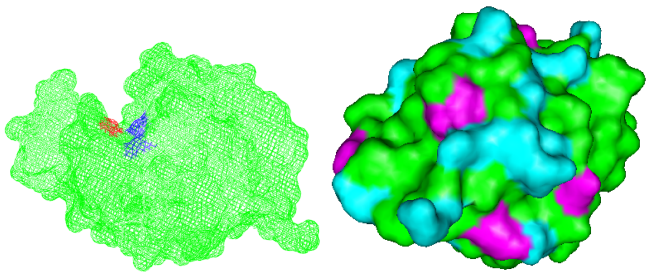

Figure 3.10: *The left image displays the active site as the "pocket" in the top right of the image. Residue Glu 35 is marked with blue and residue Asp 52 is marked with red. These two constitutes the active site. In the image to the right the saltbrigdges are displayed. The acidic amino acids, Asp and Glu are marked with magenta and the basic amino acids, Lys, Arg and His are marked with blue. The model is calculated at a pH value of 8.*

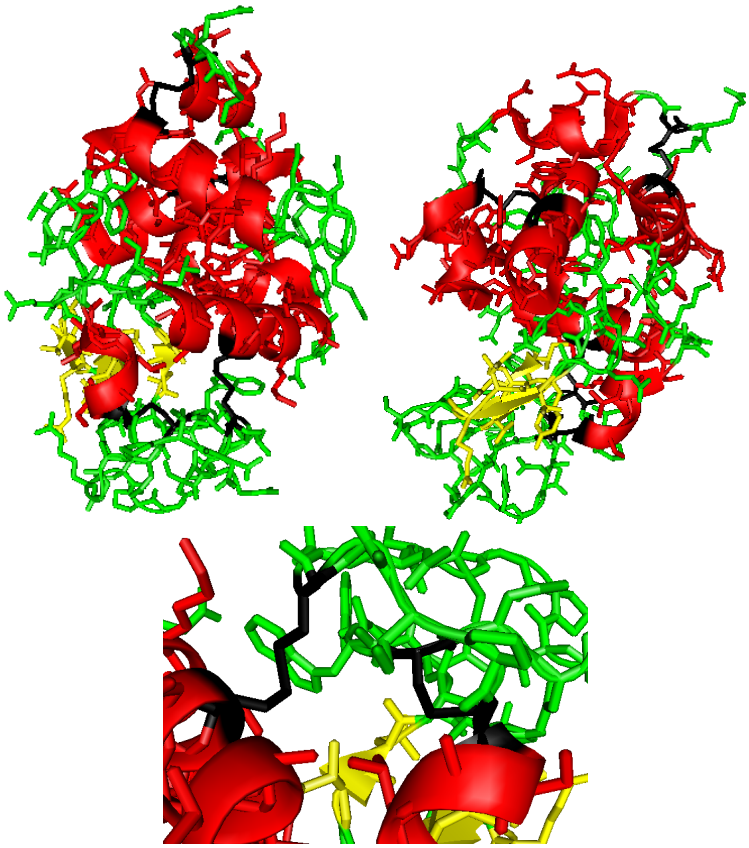

Figure 3.11: *In the two images at the top, the four disulphide bridges are shown from different angles. Cys has been marked with black to illustrate the bridges. In the bottom picture two disulphide bridges are highlighted with black.*

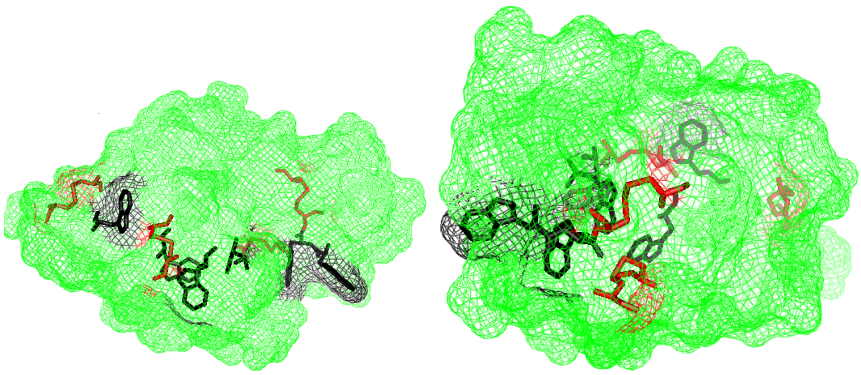

Figure 3.12: *The figures above illustrate the appearance of Trp colored black, and the disulphide bridges colored red. Five Trp are exposed on the surface and one is hidden in the center of lysozyme.*

3.5 Fluorescence Spectroscopy

The results from the fluorescence spectroscopy experiment is graphed in Figure 3.13 to Figure 3.15 . The entire set of data can be found on the attached CD.

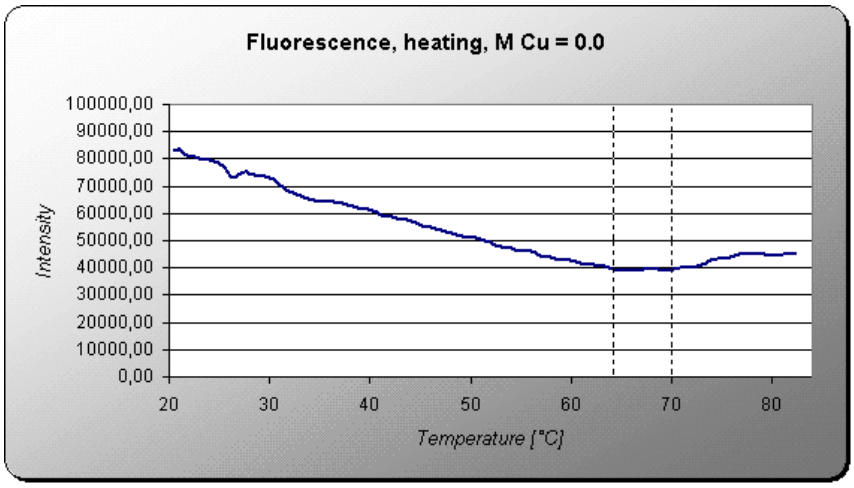

Figure 3.13: *This graph shows the denature process of lysozyme. Fluorescence intensity is measured at 350 nm. The dotted lines divide the picture into three different sections. The leftmost section illustrates the dynamic quenching, in the middle section the dynamic quenching is balanced by denaturation and in the rightmost section the quenching is surpassed by the denaturation process.*

Stern Volmer Plot

At 350nm the maximal value of intensity was observed. At this wavelenght the difference in absorbtion between the various concentrations of $CuCl_2$ is at maximum. Therefore this wavelength gives the highest accuracy possible. These data is used for the plot in Figure 3.16 and listed in Table 3.3 .

$[CuCl_2]$	Fluorescence intensity	$k_q\tau_0$
0	87372	1
0,025	85194	1.0227
0,05	84386	0.7077
0,1	80977	0.7897
0,15	77362	0.8626

Table 3.3: *The data measured at 350nm. $k_q\tau_0$ is the Stern Volmer quenching constant.*

Inserted into Equation 2.7 the data gives a $k_q\tau_0$ value at 0.842 and a equals 1.

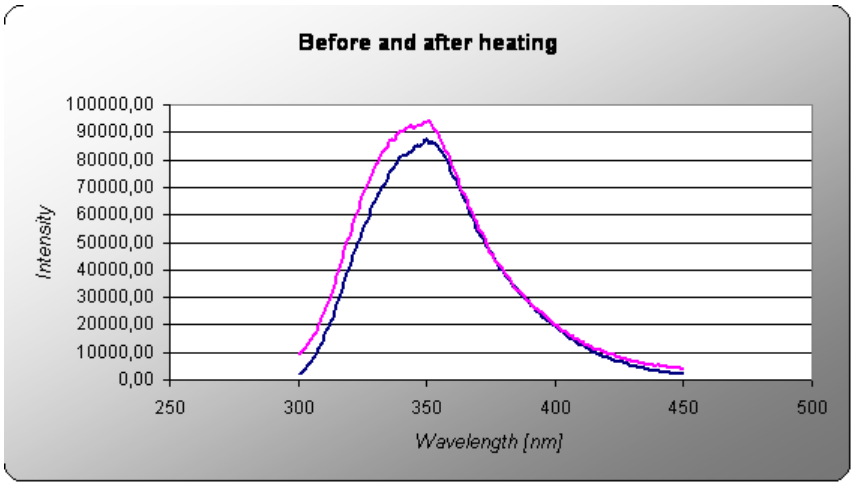

Figure 3.14: *This graph shows a wavelength spectrum of lysozyme before and after heating.*

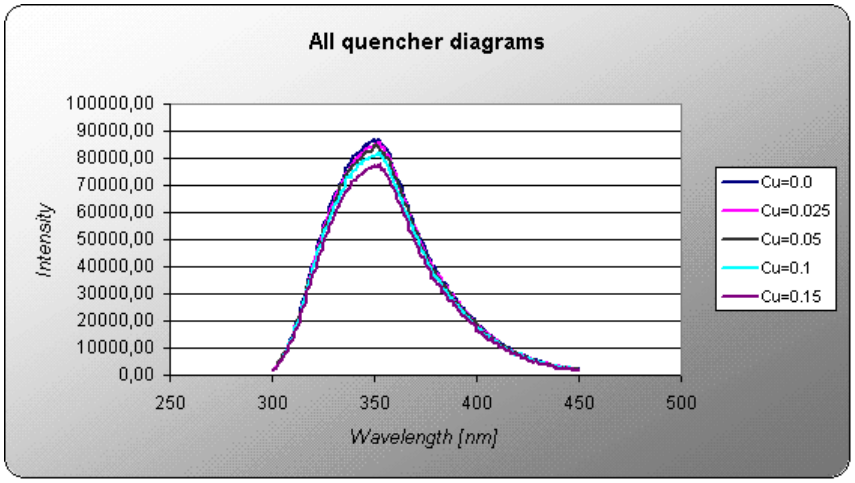

Figure 3.15: *This diagram shows the development of intensity compared to wavelength as the level of* $CuCl_2$ *increases.*

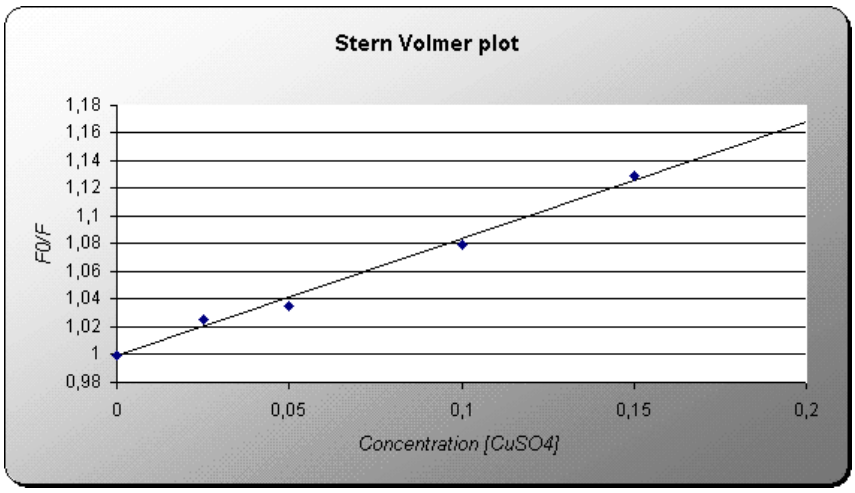

Figure 3.16: *The values calculated from the Stern Volmer equation is plotted in the graph. The black line is an approximation made using Equation 2.7 . The slope of the approximating line is 0.842.*

3.6 Circular Dichroism

The data from the circular dichroism experiment is graphed from Figure 3.17 to Figure 3.20 . The entire data set can be found on the attached CD.

Distribution of secondary structure

The result from the program k2d is illustrated in Figure 3.19 and Figure 3.20 . Furthermore the distribution of the secondary structure is listed from the computed curves under the diagrams together with the distributions from the model of the protein.

	Before	After	1DPX
Alpha	25%	9%	50.4%
Beta	19%	42%	6.2%
Random	56%	48%	43.4%
Square Distance	50.12	487.86	
Max error	0.122	0.227	

Table 3.4: *The distribution of the secondary structure, before and after heating, is estimated by the program k2d [www.embl heidelberg.de, 2004]. The distribution from the 1DPX data file is from [www.rcsb.org/pdb, 2004].*

Table 3.4 shows the distribution of the secondary structure before and after heating compared to the secondary structure for the model calculated from the structure file of 1DPX. [www.rcsb.org/pdb, 2004]

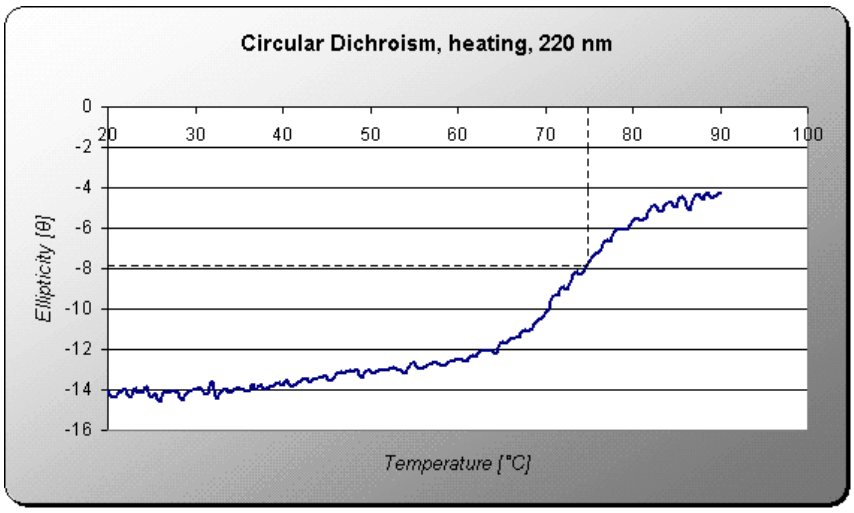

Figure 3.17: *This graph shows the denature process of lysozyme with a temperature ramp of* $1.5°$ *per. minute. The wavelength is set to 220 nm. The* T_m *value is* $75°C$*, marked by the dotted line.*

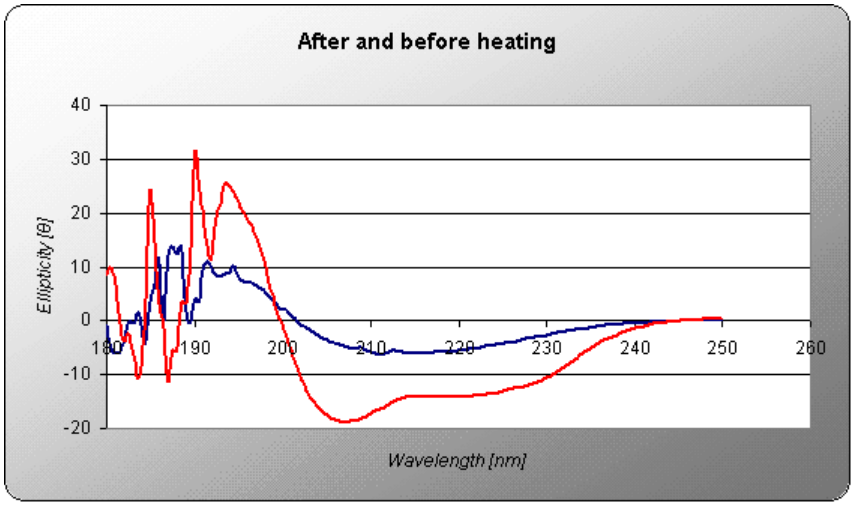

Figure 3.18: *The red graph shows a wavelength spectrum of lysozyme at* $20°$ *celsius before heating. The blue graph shows the analysis of lysozyme after cooling from* $90°C$*.*

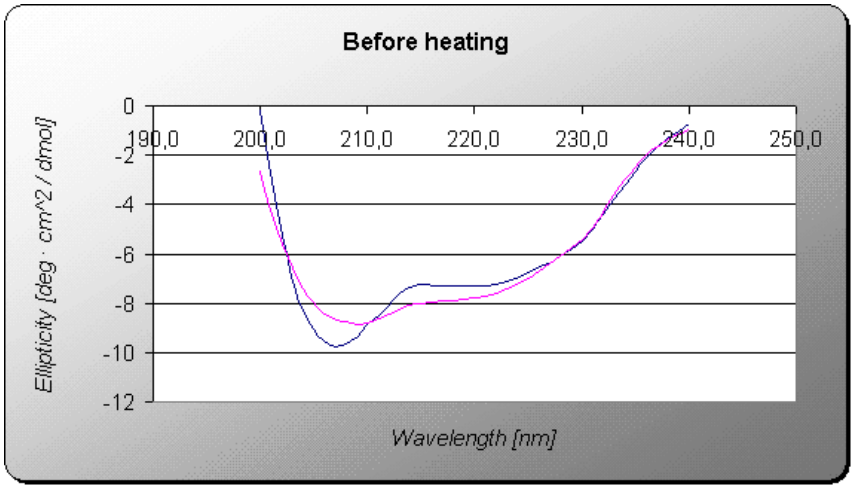

Figure 3.19: *The purple curve shows the ellipticity from the protein-solution before heating. The blue curve is the estimated curve from the program k2d.*

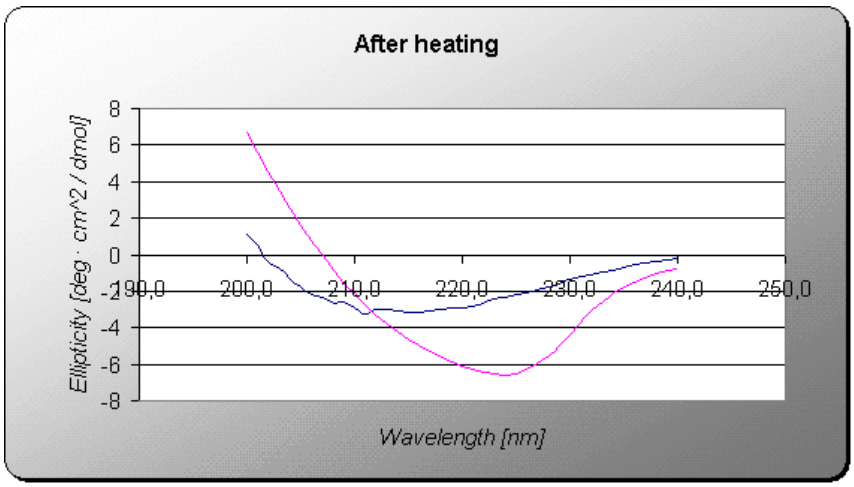

Figure 3.20: *The blue curve shows the ellipticity from the protein-solution after heating. The purple curve is the estimated curve from the program k2d.*

Chapter 4

Discussion

4.1 Crystal Growth

Protein crystal growth is a trial and error process in order to find the optimal conditions for crystallization. Therefore it is impossible to know when to expect crystals prior to the experiment.

Suitable crystals were achieved and examined in optical microscopy see Section 3.1 . These crystals could be used for X-ray diffraction and through Fourier transforms the spatial structure of proteins could be determined. X-ray diffraction was not possible to conduct because of the lack of instruments. It is not possible to use atomic force microscopy on lysozym crystals due to the lack of crystalline strength.

4.2 Optical Microscopy and Atomic Force Microscopy

Lysozyme

Optical microscopy was used to observe the lysozyme crystals and the data has been used to illustrate the crystals in a three dimensional view. The collected data from the crystallization of lysozyme was difficult to measure due to the structure of the crystals. The problem was solved by studying different crystals and from these estimate an overall model. These models are shown in Figure 4.1

Optical microscopy and Atomic Force Microscopy

Optical microscopy and atomic force microscopy has been used to measure the angles on the $CuSO_4$ crystal in two different ways. Optical microscopy is used to give a two dimensional image of the crystal, while atomic force microscopy is used to measure the vertical variation.

The data from these two methods can supply each other as they measure different angles of the same crystal. A model has been formed using the measured angles to illustrate the appearance of the $CuSO_4$ crystal in 3D, see Figure 4.2 . Crystals with oblique angles tend to have a triclinic structure.

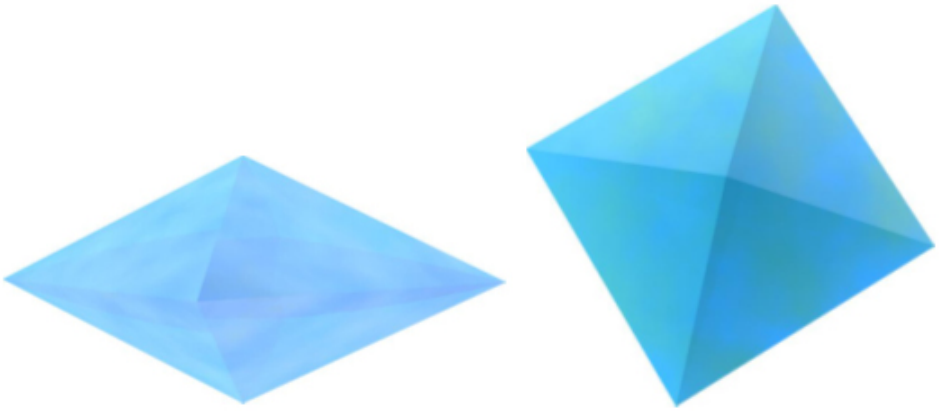

Figure 4.1: *The figure shows models of lysozyme crystals from two perspectives. The models are made using Cinema4D**TM**[www.maxon.net, 2004]*

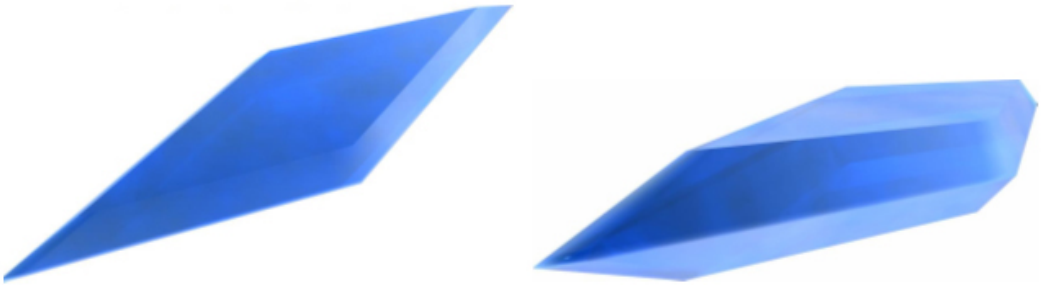

Figure 4.2: *The figures shows models of $CuSO_4$ crystals made with Cinema4D**TM**[www.maxon.net, 2004].*

Optical Microscopy of $CuSO_4$

From the optical microscopy pictures, it was possible to measure the angles of the $CuSO_4$ crystals. The validity of these measurements depends on the orientation of the crystal. This means that if the structure is tilted the appearance of the structure is changed. This would result in invalid measurements of angles but this can be diminished by basing the measurements on the frequency of the occuring angles. See Section 3.1 .

Atomic Force Microscopy of $CuSO_4$

The purpose of atomic force microscopy was to study the surface of $CuSO_4$ crystals. The atomic force microscopy graph of $CuSO_4$, shown in Section 3.4 , illustrates the topography of the crystals. Optical microscopy images can be studied without any data computation while atomic force microscopy returns a set of data. In order to visualize the topography these data must interpreted.

The atomic force microscope has some advantages compared to the optical mi-

croscope. The resolution in atomic force microscopy is, for the time being, 2 nm [Howland and Benatar, 2000], while the optical microscope is limited by the wavelength of visible light. This corresponds to a resolution at 200nm [Britannica, 2004]. Another advantage is the ability to make depth perception. The atomic force microscopy also have disadvantages. One disadvantage is the problem of tracing over an overhang. This is illustrated in Figure 4.3 .

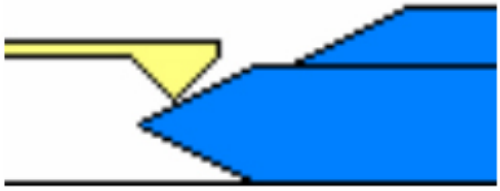

Figure 4.3: *This figure shows a tip tracing over an overhang. As it is seen the tip is not able to measure the topography under the overhang.*

The atomic force microscope produces an abstract image of the surface. This makes the relation between the surface and the graphed data vague. The high level of magnification degrades the relation between the image and the subject.

When studying the atomic force microscopy data it is possible to measure the angles of the crystal. This can assist in determining the type of crystal. At first the procedure of atomic force microscopy seems easy and straightforward, but when examining the results the angles are difficult to measure. The difficulties occurred because it was found hard to know exactly what the images show, and how the data can be related to angles in the crystal.

Another problem with the recorded atomic force microscopy data is noise. Because atomic force microscopy measures the topography on the nanometer scale, even the smallest vibrations will cause disturbances. These vibrations could be caused by a shutting door or even the vibrations in the air caused by people talking. The noise can be seen on the left side of Figure 3.4 as small vibrations. Ideally, the lines of the cross sectional view would be straight. The noise adds to the difficulties of measuring angles.

Even due to these problems angles from the atomic force microscopy data was measured. They were found to be 132° in average. This angle cannot be found in $CuSO_4$ crystal obtained by X-ray diffraction [www.database.iem.ac.ru, 2004]. According to this source the angles found in $CuSO_4$ are 82°, 107° and 102°. This inconsistency can be explained by noise or the fact that it was uncertain what exactly was being measured. This makes it even harder to relate the measurement to reality.

Roughness

Surface and area roughness parameters are meant to help determine the surface texture of a material. The analysis of the roughness gave values between 0.096 and

0.125nm.

There are two primary potential sources of error in using an atomic force microscope for measuring surface textures. The first is the probe geometry and the second is the length scale of the measurement.

The surface texture that is measured with an atomic force microscopy depends on the geometry of the probe tip. If the probe tip is larger than the features causing the surface texture, then the surface roughness measurements will appear smaller than they should be. The sharper the tip is, the smaller the error gets.

Within the image used for the surface roughness calculation there must be an adequate sampling of the features. As a result, it is possible to get a different surface texture when the scan size is changed. This problem is avoided by using the same size scan range when surface roughness on several samples is being compared. The data collected are all taken in the exact same scan range. [www.lot oriel.it, 2004]

4.3 Absorbance Spectroscopy

Absorbance spectrum 0.17 M $CuSO_4$

The solution contains ions of Cu^{2+}, SO_4^{2-}. The results show, see Figure 3.5 , that light at wavelengths in the area between 400 and 600nm is not absorbed in the solution. Actually light at wavelengths around 600nm is yellow but because the human eye is more sensitive to blue light, the $CuSO_4$ solution appears blue [www.syn.aaa.dk, 2004]. The blue color of the solution is due to the Cu^{2+} ion.

The inaccuracies on Figure 3.5 in the area below 300nm is due to the limits of the instrument.

Absorbance spectrum of $CuSO_4$ with NH_3

The solution contains ions of Cu^{2+}, SO_4^{2-} and NH_4^+. In the solution a complex of $Cu(NH_3)_4^{2+}(aq)$ is formed. This complex is deeper blue. [Mygind, 2004]

The results show, see Figure 3.6 , that the sample absorbs at a wider spectrum than the previous sample. This correlates with the color of the sample which had a deeper blue tone. In this case wavelengths in the purple and green/yellow area are absorbed.

The inaccuracies on Figure 3.6 in the area below 300nm and with absorbances above three is due to the limits of the instrument.

Transmission spectrum of $CuSO_4$ with NH_3

The results show, see Figure 3.7 , that the transmission of light from the sample takes place around two areas of the wavelength spectrum. Around the area of the blue light between 350 to 550nm and then again in the area of the infrared light above 700nm. The second area is a result of a dynamic complex between Cu^{2+}, NH_3 and H_2O which allows infrared light to pas through the sample.

Epsilon values of $CuSO_4$

The results show, see Figure 3.8 , the absorbance of $CuSO_4$ from three different experiments. The data is compensated for deviations in the conduction of the experiments with respect to concentration and path length. This is done to ensure that it is possible to compare the data. The variation in the traces can be caused by inaccurate weighing of $CuSO_{4(s)}$ and repeating use of the same cuvette without optimal cleaning. Similarities between the results supports the validity of the experiment.

4.4 Fluorescence Spectroscopy

Fluorescence heating

At first the results of fluorescence spectroscopy do not show the expected S-curve. Closer examination shows that the curve can be divided into three parts, see Figure 3.13 , from 20 to 63°C, 63 to 70°C and finally from 70 to 85°C.

In the first part, the intensity of the fluorescence is decreasing. This is a result of H_2O acting as a quencher and while the temperature is rising the particles are moving faster. The rise in kinetic energy results in an increased amount of collisions and thereby collisional quenching. In this part the protein is still stable.

In the second part the enzyme is becoming unstable and the denature process begins. The disulphide bridges functions as static quenchers when located near the fluorophores. See Figure 3.12 for an understanding of the structure. The denature process removes the disulpide brigdes from Trp resulting in decreased quenching effect.

The third part is formed like an S-curve this is where the enzymes denature process is accelerating. In this part the quenching effect of H_2O is overruled due to the decreased static quenching and the exposure of Trp to the solution. This results in a higher intensity of fluorescence at $350nm$. In this part the T_m value is found and estimated to approximately 74°C. For a precise value it is necessary to carry out the experiment several times. Furthermore, if the curve can be mathematically approximated, it is possible to determine the T_m value for the enzyme by finding the zero value of the second derived function.

Before and after heating

In Figure 3.14 the graphs before and after heating are compared. This shows that the unfolding process is not reversible. When a protein solution is heated and afterwards cooled slowly the salt bridges are not able to rebind properly.

If the concentration of protein is high, the unfolded proteins will interact with each other, get to heavy to be suspended in the liquid and instead precipitate. With a lower concentration, the probability of proteins refolding instead of interacting with each other is higher. The correct bondings will be reformed.

If refolding takes place there is a probability of the secondary and tertiary structure being invalid. Thereby causing the enzyme to loose its catalytic ability.

Quencher diagrams

From the quenching diagram, see Figure 3.15 , it is clear that the concentration of the quencher has an effect on the fluorescence intensity. If the concentration of a quencher is rising the fluorescence is falling.

The Stern Volmer constant has been calculated to 0.842 as seen in Section 3.5 using Equation 2.6 . The Stern Volmer constant has also been calculated as 0.651 [A303, 2004] and 1.150 [A304, 2004]. The variation can be explained by the inaccuracies of the experiment.

Visualization in relation to Fluorescence Spectroscopy

The fluorescence spectroscopy results showed that the static quenching is decreased as the lysozyme is denatured. This indicates that there must be disulphide bridges situated near Trp in order to function as static quenchers. This is confirmed by the visualization, see Figure 3.12 .

The visualization shows one Trp buried inside lysozyme, but this information is impossible to conclude directly from the graphs. The emission from this Trp is lost in the increase of fluorescence from the five surface exposed Trp.

4.5 Circular Dichroism

Circular Dichroism, heating

The results show an S-curve, see Figure 3.17 . The T_m value is estimated to 75°C with the same procedure as in Section 4.4 . It would be advantageous to carry out the experiment several times to eliminate the interferences in the data. The value found in Section 4.4 is 74°C which matches this value.

Before and after heating

The results shows that the secondary structure is damaged due to heating, see Figure 3.18 . This can be seen from the difference in the absorption of circularly polarized light. Measurements in the area below 195 nm are invalid which is a result of worn down mirrors in the circular dichroism instrument.

The calculated distribution of the secondary structure shows that the concentration of α-helix is decreased after heating. This was expected in coherency with the data from fluorescence spectroscopy, which shows that the unfolding process was not reversible. The concentration of β-sheets is increased after heating and random coil is decreased. This was not expected as the unfolding is not reversible.

The k2d program, [www.embl heidelberg.de, 2004], compares the data to a list of 16,900 different distributions of secondary structure. Using this program and the

data from the experiments we have calculated and graphed distributions of secondary structures. These estimated distributions does not match the ones found in the lysozyme database file Table 3.4 . This is partly due to inaccurate measurements as mentioned earlier and partly due to incompletement in the data sets of the k2d program. When comparring the graph from the measured values and the graph after the k2d calculation there is a mismatch, see Figure 3.19 and Figure 3.20 . This will result in a wrong distribution of secondary structure. Conclusively the program is not able to calculate a precise distribution with data of this inaccuracy in the case after heating.

The k2d program uses the square distance as a measurement of inaccuracy. This value is large after heating which means that the estimations of secondary structure are invalid. This can also be seen from the amount of random coil, which decreases.

Visualization in relation to Circular Dichroisme

The visualization data verifies that α-helix, β-sheets and random coil are present in the enzyme. Using the data from circular dichroisme it is not possible to determine the amount of the different classes of secondary structure. This is shown in the database file which makes visualization a useful tool.

4.6 General discussion on theory, data and models

Often it is easy to make scientific experiments and obtain huge amounts of data. The problems begins when analyzing the data. First of all some data may be useless, and it is important to understand how to sort the invalid data from the valid data. When this task is completed the next challenge is to interpret and translate the data into an understandable result. This is done using knowledge about how the outcome of the experiments might be, based on theory on the subject. It is important to understand the various models that describe reality. However, when the data has been analyzed and understood, certain errors in connection with the existing theory might occur. To deal with these deviations it might be useful to know different approaches to understand theory and experiments. Through history there has been several approaches to the task of understanding experiments in connection with knowledge. There are differences between accepting experiments as science and to see them as verifications of the known theory. This contrast between the theory and the experiments is important. In the world of physics it is understood that the difference must be explained by errors in the experiment. The reason is that physics is described as an exact science. This means that the laws of physics are seen as an exact illustration of how the world functions. If a result from an experiment is wrong, it means that the experiment is wrong. This approach to sciences is known as logical positivism. In physics the theories are based on a rationalistic point of view where people who believe in theory and not in experiments are known as rationalists. Rationalism as a philosophical view regards reason as the chief source and test of

knowledge. Not experiments or tests. This is why we trust Newton's laws to hold the truth.

An opposing example is biology, here the exiting theory is based on empirical research, meaning that the world is understood by experiences gained through the senses.

In this specific project, and in connection with nanotechnology in general, several different approaches to theory and models have to be used. An example is the data obtained from circular dichroism, the way of analyzing the data was to compare them to a large number of known results and thereby determining the distribution of the secondary structure. This approach is building directly on comparing empirical data. In contrast, the fluorescense spectroscopy data was analyzed using a known formula to find the Stern Volmer constant.

Chapter 5

Conclusion

The general purpose with this project was to gain knowledge about the procedures of problem orientated work. The secondary goal of the project was to obtain experience about different techniques in connection with analysis of structures on nanoscale. During the project a number of different techniques have been studied. Thereby experience in the fields of structure analysis has been achieved. From the experiments it has been concluded that work on the nanoscale is complicated because direct observation is not possible.

5.1 Optical Microscopy and Atomic Force Microscopy

Optical microscopy is a way to examine objects, such as crystals and cells of the human body. In nanotechnology, however, it is not usable because the magnification is limited by the diffraction of light. Therefore it is only used for preliminary work.

Atomic force microscopy is a tool for examining micro and nano structures. The data produced from the atomic force microscope is a challenge to interpret, as it is difficult to separate the noise from the data. Furthermore it requires a certain experience to seperate valid data from invalid data. The atomic force microscope has been used to measure angles and determine the roughness of the scanned surface. It is, however, difficult to conclude on the data. The roughness is not useable in this case because it requires commensurable data.

The angles can be used to determine the crystal structures. Combined data from optical microscopy and atomic force microscopy has resulted in the conclusion that $CuSO_4$ crystals has a triclinic structure.

5.2 Absorptions Spectroscopy

The method of absorptions spectroscopy can be used to determine the concentration of different chemical solutions. In this context the method gave knowledge about the principle of how light is absorbed in and transmitted from a solution.

5.3 Fluorescence Spectroscoopy, Circular Dichroism and Visualization

Fluorescence spectroscopy is a tool to analyze the surroundings of fluorophores in macromolecules. This method has the ability to follow the thermal unfolding process. The problem with this method was that the heating curve was interfered by the quenching effect of H_2O.

Circular dichroism is another tool to analyze protein structures. The data collected through circular dichroism can be used to show that the protein contains α-helix, β-sheets and random coil and can, like fluorescence spectroscopy, monitor the thermal unfolding process. If the data had been valid in the spectrum 180 to 200 nm, it could have been used to determine the quantity of the different types of secondary structure in the specific protein, using commercial software instead of k2d.

Fluorescence spectroscopy and circular dichroism complements each other in the analysis of proteins. These two methods were used to determine the T_m values. Furthermore they were used to decide the reversibility of the unfolding process. It was concluded that the unfolding was not reversible.

To get an understanding of the two previously described methods, visualization can be used. Visualization is not a method but it gives a detailed model of the protein. Conclusively this gives an understanding of the native protein in different environments.

Chapter 6

Putting into perspective

After a time consuming process using circular dichroism, fluorescence spectroscopy, atomic force microscopy, absorbance spectroscopy and optical microscopy, it was found that the collected data gave little information about the structure of Lysozyme and $CuSO_4$. This was, however, not the main goal of the project, but it gave a picture of how scientists work.

The groups working on this project has collected and processed a lot of data. Parts of the results were invalid. Valid results require repetition of the experiments to ensure scientific acceptance. A more specific project would not involve both lysozyme and $CuSO_4$. It would be an advantage to eliminate one of the subjects in a new project.

If more time was available, work with other methods such as dynamic light scattering, differential scanning calorimetric and X-ray diffraction, in connection with analysis of lysozyme, would have been conducted. Activity measurements of lysozyme using absorbtions spectroscopy would also be relevant. If the circular dichroism experiment was to be reconducted, the mirrors would need replacement, as they were worn down.

As mentioned it would not be ideal to work with many different methods, but the main goal of this project was to gain knowledge about the different techniques of structure analysis. In a new project with focus on $CuSO_4$, other types of scanning probe microscopy would have been used. X-ray diffraction and electron microscope would also be interesting techniques to use for structure identification.

Appendix A

Crystal Growth

Basically crystal growth is a simple process and can often be achieved by cooling a hot saturated solution of for example kitchen salt, $NaCl$. That is when dealing with simple molecules of inorganic substances. Even polar organic substances can be crystallized by a similar process.

Complex organic molecules such as proteins cannot be crystallized using a process similar to this. To proteins this technique would result in denaturation simply due to the heat. Another technique must be utilized along with a set of parameters strictly maintained.

First it is necessary to assure the purity of the protein. By that meaning presence of other substances and the uniformity of the surface properties of the protein, hence the protein folding dependency. Once dissolved in a suitable solvent another set of parameters are put into play. The solvent normally consists of a water-buffer solution sometimes with an organic solvent or precipitant. [Drenth, 2002]

Techniques

One widely used technique is vapor diffusion utilizing a heterogenic equilibrium between the precipitant solution and the protein solution. See Figure A.1 for the set up of the hanging and sitting drop method. Drops of a mixture of protein and precipitant solution, to an extend where no precipitation will occur, are placed on a microscope slide. The slide must be siliconized for the drop not to spread and it is placed on top of a pit filled with the precipitant solution [Rhodes, 1993]. The parameters of the precipitant solution are the ones up for investigation. When using $NaCl$ as the precipitant the equilibrium in Equation A.1 is found.

$$H_2O(l - precipitant) \leftrightarrow H_2O(g) \leftrightarrow H_2O(l - drop) \tag{A.1}$$

The amount of buffer solution is by far larger than the protein solution resulting in a slow increase of $NaCl$ concentration in the protein solution. Note that the $NaCl$ concentration in the buffer is not altered noteceably. The equilibrium which is initially offset to the right will slowly displace to the middle by transferring H_2O

to the protein solution. According to the Debye-Hückel theory for ionic solutions the proteins will often not solute without any $NaCl$ but when an amount is added the proteins will solute due to the salting in effect. Continual increase of $NaCl$ concentration will bind the water to the dissolved $NaCl$ and cause the protein to precipitate.

This technique makes it possible to reach a fixed set of solution parameters slowly without manually adding substances to the protein solution. Therefore it enables a larger amount of experiments saving time finding the optimal crystallization parameters.

If the surface tension of the protein solution is not sufficient for the hanging drop method a method called the sitting drop may be utilized see Figure A.1 .

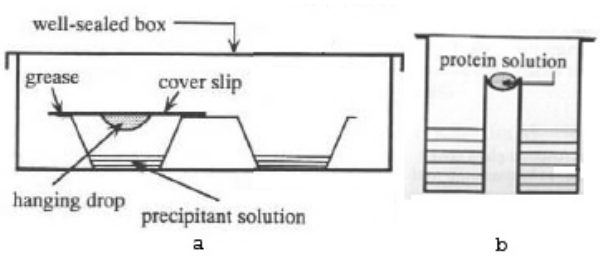

Figure A.1: *The vapour diffusion technique utilized in both the hanging(a) and sitting drop(b) method. There is a diffusion between the precipitant solution, the vapour and the drop resulting in an equilibrium [Drenth, 2002].*

Besides the vapor diffusion technique there exists the liquid-liquid diffusion and dialysis. The liquid-liquid and the vapor technique are quite similar, each one utilizing a heterogenic equilibrium, the liquid-liquid being as the name implies between two liquids of different density. In the dialysis technique the protein and precipitant solutions are divided by a membrane [Drenth, 2002].

The protein crystallization may result in many small crystals instead of the desired large single-crystals that can be used for X-ray diffraction. This can be avoided by using small crystals of good quality as seeds in the protein solution. The crystals will grow on the surface of the seed and may grow up to ten times faster. The seeds may be used independent of the crystallization set-up. [Rhodes, 1993]

The parameters of the precipitant and protein solution are dependent on the nature of the protein. Some proteins contain hydrophobic surface areas, often connected to the interior of membranes, and are not soluble in aqueous solutions. This can be avoided by adding a detergent that will function as a coating to these areas and allow it to dissolve.

Conclusively protein crystallization is a trial and error process. It is necessary to test a large number of parameters in order to find the optimal crystallization conditions. But since a large single crystal is crucial to X-ray crystallography and thereby to the determination of the spatial structure of the protein it is important to find the optimal conditions.

Optimization of parameters

With a series of experiments it is possible to mathematically optimize the crystallization conditions. Forming a function with respect to the different parameters for example f(pH, Temp, concentration of protein and other additives) and letting f be a value of the ration between the shortest and longest distances in the protein. A large value of f will then imply a three dimensionally large crystal while needle shaped crystal will obtain a smaller value. Even though it is not possible to find an expression of f it is possible to find an approximation of the multidimensional function. Using a mathematical program it is possible determine the location of peaks implying optimal conditions and a guideline for the next generation of experiments. [Rhodes, 1993]

Crystalline protein structure

Another problem must be addressed when crystallizing proteins. The main cause of the proteins functionality are their spatial structure. The key question one need to ask is "are the spatial structure maintained while crystallizing proteins? ". Since it is not possible to examine the structure with X-ray crystallography before the crystallization process other indices are needed. One significant argument is that many proteins maintain their function in the crystalline state. When a crystallization of enzymes are exposed to substrate they continue to convert the substrate into products in a slower rate due to less availability. Other methods of structural determination such as the NMR-scan can be utilized and compared to the data from the X-ray crystallography. In most cases the two models are almost identical and the best likeness are in the α-helices and the β-sheets although they vary a little in the surface loops. [Rhodes, 1993] In many cases two different crystals of the same protein have resulted in identical X-ray diffraction scans indicating that the crystallized protein are of the same spatial structure as in the solution.

Finally one should bear in mind that the proteins, both the dissolved and the crystallized, contain a large amount of water molecules that helps stabilizing the proteins spatial structure. This implies that the proteins although crystallized are still to some extend in an aqueous state. If the water is removed, the protein structure will alter.

Appendix B

X-ray Crystallography

History behind X-rays

X-ray radiation was first discovered by Wilhelm Conrad Roentgen on the 8th of November 1895, but because the nature of such radiation was not yet understood, Roentgen called them X-rays. In 1910, Max von Laue developed a theory on X-ray diffraction by a three dimensional lattice. This inspired his two assistants, Walter. v. Friedrich and Paul Knipping, to use a crystal as a diffraction grating. Their results were published in 1912 and their findings were direct proof of the existence of lattices in crystals and the wave nature of X-rays. [Drenth, 2002]

X-ray sources

The main hardware needed for the collection of X-ray diffraction data is an X-ray source and an X-ray Detector. X-rays are electromagnetic radiation with wavelengths between 1000 and 0.1 Å.

The most common X-ray device is the sealed X-ray tube, because it is easy to use and give fine results for preliminary work especially on smaller proteins. In the sealed tube a cathode emits electrons. The tube is under vacuum and the cathode has high negative potential with respect to the metal anode, the electrons are accelerated and reach the anode at high speed. For protein diffraction the anode is usually a copper plate, were the electrons are focused onto an area of $0.4 \cdot 8mm$. Most of the electron energy is converted into heat. However a small part of the energy is emitted as X-rays in two different ways. One as a smooth function of the wavelength, this continuous region is due to the physical phenomenon that accelerated charged particles emit radiation called "Bremsstrahlung". This region has a sharp cut-off, at this edge the X-ray photons obtain their full energy from electrons when they reach the anode, see Figure B.1 The sharp peaks in the spectrum are due to electron transition between inner orbitals in the atoms of the anode material. When the high-energy electrons from the cathode reach the anode they shoot out electrons from low laying orbitals, electrons from higher orbitals falls to the lower orbitals thus emitting X-rays. One problem with the fixed anode is that the heating caused by the electron beam at the

focal spot can ruin the anode and that limits the maximum power of the tube. This limit can be moved by using a rotating anode tube. The advantage over the sealed tube is higher radiation intensity, but a disadvantage is that it requires a continuous pumping to keep the vacuum at the required level. [Drenth, 2002]

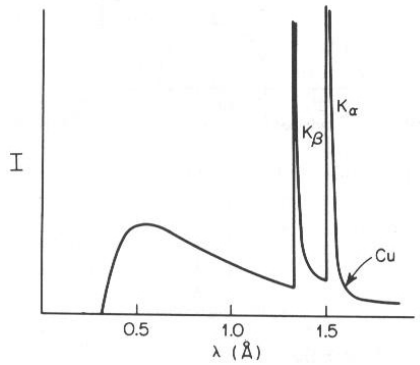

Figure B.1: *The spectrum from an X-ray tube with a copper anode. It shows a continuous spectrum and in addition two sharp peaks due to quantized electrons in the copper. I is the energy of the emitted radiation on an arbitrary scale [Drenth, 2002].*

Synchrotron Radiation

Particle accelerators as synchrotrons and storage rings are the most powerful X-ray sources. Because protein molecules are large, their crystals diffract X-ray beams much less than crystals made of small molecules. The reason for this, is that the diffraction is a cooperative effect between the molecules in the crystal. With larger molecules there are fewer units needed to make a crystal of the same size than if it consisted of smaller molecules and therefore the diffracted intensity is lower. Also proteins mostly consist of C, N and O atoms and these are light elements with only a few electrons (6-8) per atom. Since the electrons are responsible for the scattering of the X-rays the light elements does this more weakly than atoms with more electrons. Because of this relatively low scattering, protein crystallographers prefer to use a high intensity source, such as a rotating anode tube. For crystals below 0.1 mm or with extremely large molecules, synchrotron radiation is required for data collection. Synchrotrons are devices used for circulating electrically charged particles at nearly the speed of light. The particles are injected into a storage ring directly from a particle accelerator or a synchrotron booster. The electrons are kept in the storage ring with electro magnets. When the particle beam nears the magnets they change direction (and is kept in the ring) and thereby the electrons or positrons emit electromagnetic radiation. The synchrotron radiation is highly polarized and continuous. Its intensity and frequency are directly linked to the strength of the magnetic field and the energy of the charged particles affected by the field. That means, the stronger the magnetic field and the higher the energy of the particles,

the greater the intensity and frequency of the emitted radiation. [Drenth, 2002]

Cameras and Detectors

Image plates are used for collecting data from diffraction. Image plates are made by depositing a thin layer of an inorganic storage phosphor on a flat base. The X-ray photons excite electrons in the material to a higher energy level. Part of this energy is emitted almost immediately as light in the visible area. However, an appreciable amount of energy is retained in the material in a period of several days, but is slowly dissipated. The retained energy can be released by exposing it to light. Normally a red laser is used to scan the image plate and blue light is emitted, the red light is then filtered and the data is collected by a photomultiplier. [Drenth, 2002]

Area detectors is the term used for electronically based photon detectors. They can process the data they collect instantaneously. They are also called position sensitive detectors, because they can measure both intensity and position of the diffracted beam. The area detectors measures diffraction every 0.1° this means that it is possible to make a three dimensional diffraction picture. In contrast to the image plate where larger oscillation angles are used, for example 2°, and therefore no profile is obtained for the diffraction spot in the oscillation angle. Area detectors are based on either a gas-filled ionization chamber or an image intensifier coupled with a video system or Charge Coupled Device (CCD). In the absorption gap X-ray photons cause ionization of gas atoms with the formation of ions and electrons. The liberated electrons ionize neighbouring gas atoms by collision with the result that about 300 ions and electron pairs are formed by absorption of a single 8keV ($\lambda = 1.55$)Å X-ray photon [Drenth, 2002]. It is not enough for a measurable signal, so the signal is amplified and measured between an electric field of an anode and a cathode. This kind of diffraction detector has a disadvantage referring to synchrotron radiation due to lower sensitivity at shorter wavelengths there is poor X-ray photon absorption in the gas. In video-based area detectors the diffraction pattern is collected on a fluorescent screen. The remanent light is amplified with an image intensifier and stored in the target of a video camera tube. Then its read out and fed to a computer. Though the electronic noise is rather high it can be kept under control by keeping the system on constant temperature. Also the video camera tube can be swapped with a CCD thereby gaining a high dynamic range, combined with excellent spatial resolution, low noise and high maximum count rate. [Drenth, 2002]

X-ray diffraction

After having exposed the crystal to the X-ray radiation the X-ray is diffracted and collected. The data is collected as diffractions spots. With help from the inverse Fourier transform (will not be further discussed) the diffraction pattern can be deciphered and converted into an image of the subject. If the diffraction is not suitable enough it can be refined with the use of heavy atom replacement (will not be discussed further). With computers the collected data can be processed into 3D and

thereby be made visual see Figure B.2 . This is a good tool to study proteins etc. [Nolting, 2004]

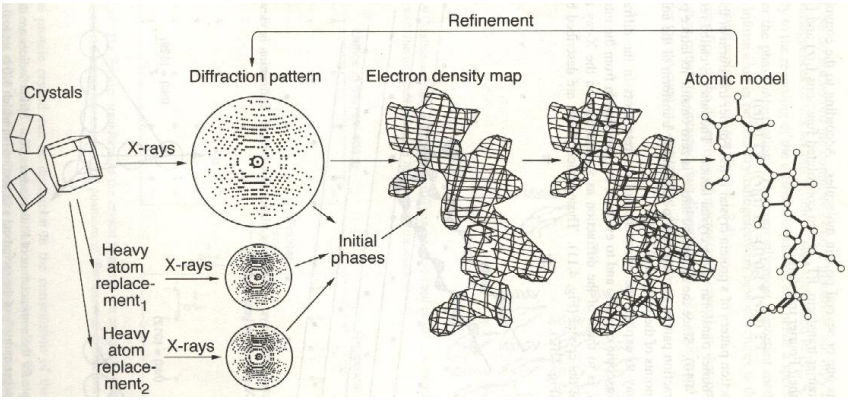

Figure B.2: *Overview of X-ray crystallographic analysis of proteins: From the measured diffraction pattern of suitable native and, if necessary, heavy atom replaced crystals, an initial electron density and atomic is calculated. The initial model is refined for example, by modifying it till its calculated diffraction pattern matches the measured pattern [Nolting, 2004]*

Appendix C

Scanning Probe Microscopy

C.1 What is Scanning Probe Microscopy?

Scanning probe microscopy, or SPM for short, is a common designation for microscopes based on the principle of a tip being traced over a surface in a raster pattern, producing a detailed visualization of the surface. The tip is mounted on a cantilever with a length of approximately 200 μm. The distance between the tip and the surface is 1 to 2 nm [Birdi, 2003]. Unlike traditional microscopes, as the optical microscope or electron microscope, SPM does not function by shooting beams of light or electrons at the sample, and then analyzing the reflections. With SPM the vertical movement of the tip over the two dimensional surface, directly translates to a three dimensional image of the surface.

Scanning Probe Microscopy has been developed for analyzing surfaces of various kinds. Ever since mankind has known about atoms and molecules, we have been wondering what they look like and what characterizes them. SPM has brought us closer to answering these questions. The picture in Figure C.1 was taken using an STM microscope. It clearly shows the individual atoms of an unreconstructed nickel surface.

SPM is a wide group under which belongs different microscopes, including the scanning tunneling microscope (STM) and atomic force microscope (AFM). Every one of these individual microscopes tell something about different properties of the sample. AFM, for example, gives data on the height profile of the sample. The construction, principles, applications and perspectives of SPM will be described in the following sections. [Birdi, 2003]

Types of Scanning Probe Microscopy

As stated in the last section there are many different sorts of SPM. Among these are STM and AFM. Many of them can be further divided into different modes of operation. This applies for example to AFM which operates in one of three modes.

The STM is the forefather of scanning probe microscopes. It was the first of its kind and was originally invented by Gerd Binnig and Heinrich Rohrer in 1982,

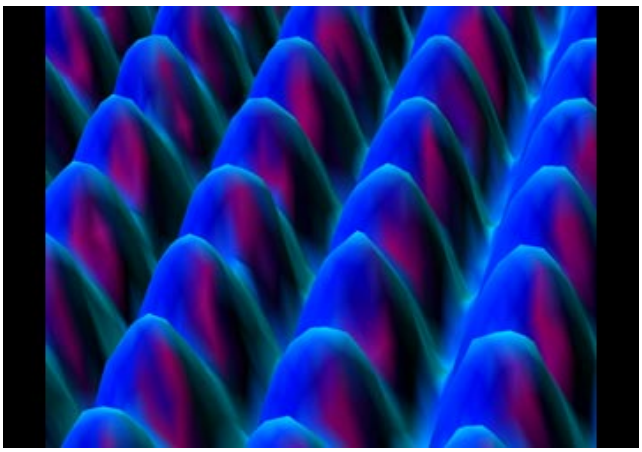

Figure C.1: *An STM picture of unreconstructed blue nickel [nobelprize.org, 2004]*

for which they were awarded the Nobel Prize in 1986 [Birdi, 2003]. STM is based on the quantum mechanical effect called tunneling. This effect depicts that there is a probability that a particle with energy E_{part} crosses a barrier, even though the energy, E_0, needed to cross that barrier is higher than the energy E_{part} of the particle. The probability, however, is not very large for E_{part} being much smaller than E_0, and it is exponentially dependant on the tunneling distance. The STM makes use of this extreme sensitivity to distance. The tip to sample separation is in the order of 5-10 Å [Birdi, 2003], which allows tunneling of electrons to occur when a voltage is applied between the tip and the sample. When the tip is scanned over the surface, variations in surface topography result in variations in the tunneling distance and therefore variations in tunneling current. This information can be processed to produce topographical images of the surface.

Another type of SPM is the scanning electron microscope. This microscope works by aiming very narrow focused beam of electrons at a specific spot on the sample. This will produce high energy back scattered electrons and secondary electrons ripped loose from the surface of the sample. The intensity of these electrons are measured and used to produce a map of the surface.

C.2 Atomic Force Microscope

Atomic force microscope is one of the most popular and useful SPMs. It operates on simple principles to gain data about the differences in height in the surface of a sample.

The Birth of Atomic Force Microscope

One of the biggest disadvantages of STM is that it can only be used on conductive samples. If the sample is nonconductive there can be no electron tunneling between

the tip and the sample, when a voltage is applied between them. Soon after the STM was invented, it was clear that another type of SPM, which allowed for nonconductive samples, was needed. This resulted in the AFM which was developed 5 years after the introduction of STM [Birdi, 2003].

Principles of Atomic Force Microscope

AFM is based on much of the same principles as STM except that AFM does not use the tunneling effect to measure surface topography; instead it uses forces between the tip and the sample. When the tip is exposed to forces, it causes the cantilever to bend and this bending can be measured and processed to create a topographical image of the surface. Several forces typically contribute to this bending of the cantilever. The force which is most often associated with AFM is the Van Der Waals forces. Van Der Waals forces is an attractive force. When the tip to sample seperation approaches zero, the repulsive force is caused by a combination of columb forces and overlapping electron clouds. Figure C.2 shows the force as a function of distance.

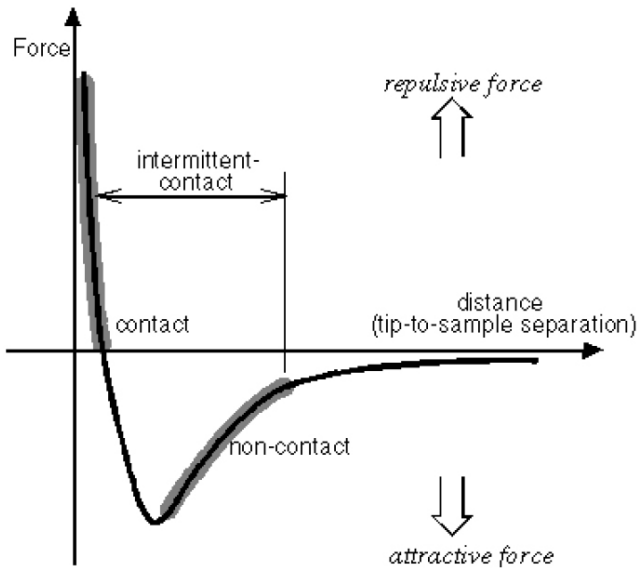

Figure C.2: *This picture shows the relationship between force and distance. In the left side of the diagram the force is repulsive caused by columb forces and overlapping electron clouds. In the right side the force is attractive caused by van der Waals forces.*

The curve clearly shows the regions in which the force is repulsive and those in which it is attractive. AFM operates in both the contact region, which is often called Direct Contact AFM or DC-AFM, and the non-contact region also called NC-AFM. Another mode of AFM operates in the intermittent-contact region, and this is called

IC-AFM. Which mode is preferred depends on the situation as will be described in the following sections. One of the main advantages of the AFM technique is the power of magnification and resolution. While optical microscopy is limited by the wavelength of visible light, the AFM is not. The resolution of an AFM is determined by the size of the tip, the step length and the step size of the image. The AFM instrument accessible, has an resolution of 15 nm [www.nanosurf.com, 2004]. With STM atomic resolution is possible.

Contact AFM

In this mode of AFM, the tip is situated in the contact region shown on Figure C.2 . The principle in this mode of operation can largely be compared to the old record player, where a sharp metal needle moved on top of a vinyl record to reproduce sound [Birdi, 2003]. The vertical movement of the metal needle directly translated to sound, in DC-AFM the deflection of the cantilever directly translates into a topographic image of the surface. The deflection of the cantilever is due to overlapping electron clouds, and the columb forces which are experienced in the contact region. When the atoms of the tip and the sample are brought close together, below 1 nm [Howland and Benatar, 2000], the electron clouds of the tip and sample atoms repel each other, and thereby cause the cantilever to bend. The magnitude of the deflection is determined by the cantilever spring constant, and generally has to be lower than the spring constant between atoms in the sample which is in the order 10 N/m [Howland and Benatar, 2000]. If the spring constant of the cantilever is larger than that of the atoms in the sample, a deformation of the sample might occur.

Detection of the cantilever deflection is done with the help of a position sensitive photo detector or PSPD for short. A laser beam is focused at the cantilever and the reflection reflects the deflection of the cantilever as shown in Figure C.3 .

When a deflection is registered by the PSPD, two modes of operation is of choice. The AFM can either be operating at constant force or constant height mode. In constant force mode the deflection causes a feedback system to adjust the height of the cantilever, keeping the force constant. As soon as the force increases the height of the cantilever is increased as well, to keep the force constant. In constant height mode, the height of the cantilever is kept constant and the deflection of the cantilever varies with the surface topography. In constant force mode, it is the up and down movement of the cantilever which produces the image, whereas in constant height mode, it is the deflection which directly produces the image.

Non-Contact AFM

This mode of AFM differs from DC-AFM in that it operates in the non contact section seen on Figure C.2 . The driving force in the non-contact region is the Van der Waals force. Where DC-AFM has the probe situated at a distance below 1 nm from the sample, NC-AFM has the probe at a distance of 10 to 100

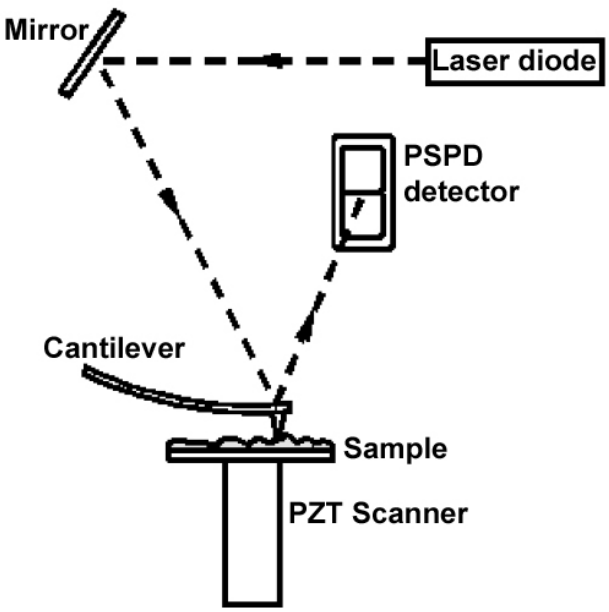

Figure C.3: *The PSPD device. The light is being reflected from the cantilever and the deflection of the cantilever can be detected. The longer the distance from the cantilever to the PSPD device, the larger angle.*

Å from the sample [Howland and Benatar, 2000]. The cantilever is vibrated near its resonant frequency with an amplitude of 10-100 Å using a piezo electric device [Howland and Benatar, 2000]. This vibration is disturbed when the tip approaches the sample, and this can be used to measure the topography of the surface. When the system detects a change in amplitude, it moves the cantilever up or down to keep amplitude constant. This up/down movement can be used to create an image of the surface, in the same way as with constant force DC-AFM.

Appendix D

Absorption spectroscopy

Spectrometers are instruments that generate, examine or record spectra. The lenses of the instrument focus light, while a central prism splits the beam into a spectrum of its constituent colors. The colors appearing on the screen represent the wavelengths that the sample did not absorb. The absorption spectra of the sample are an expression for is ability to absorb light as a function of the wavelength. Figure D.1 shows a simple line-up of an absorption spectrometer. [Serway and Beichner, 2000] In a spectrometer the transmission is recorded as a function of the wavelength of light. From this point the absorbance can be calculated using Beer-Lambert's law:

$$I = I_0 \cdot 10^{\epsilon c l} \tag{D.1}$$

I is the measured intensity, I_0 is the input intensity, l is the path traveled by the light in the sample, c is the concentration and ϵ is the molar absorptivity. The absorbance A is thereby defined as:

$$A = I_0 Log_{10}(\frac{I_0}{I}) = \epsilon c l \tag{D.2}$$

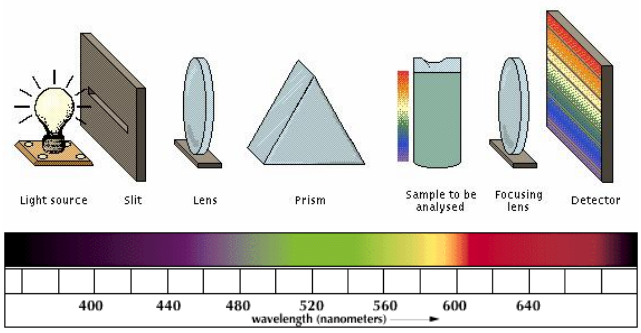

Figure D.1: *A simple line-up of a absorption spectrometer is shown. [Encarta, 2003]. Underneath a continuous-emission spectrum from an ordinary incandescent lamp is shown [Britannica, 2004]*

Appendix E

Fluorescence Spectroscopy

E.1 Introduction to Fluorescence Spectroscopy

During the last 15 years fluorescence spectroscopy has been a well known technique and is today used as a research tool in microbiology, biochemistry and biophysics. It turned out that these techniques are useful in environmental monitoring, clinical chemistry, DNA sequencing and analysis of proteins. The knowledge of fluorescence is not new. In 1845 Sir John Frederick William Herschel described the first observation of fluorescence from a quinine solution in sunlight. Unfortunately, Sir John F. W. Herschel did not continue his research into fluorescence and only published a few papers about this subject. Another important person in this context is Alexander Jablonski. Alexander Jablonski was an Ukrainian scientist who completed a remarkable research into the studies of atomic and molecular physic. His work lead, among other things, to the Jablonski diagram, which explain the processes that occur in fluorescence. [Lakowicz, 1999].

E.2 The principle of Luminescence

To explain fluorescence it is advantageous to start explaining luminescence because fluorescence is a part of it. Luminescence is the emission of light from any substance and it occurs when electrons in the excited states fall back to the ground state under emission of a photon. Luminescence is divided into two sub categories; fluorescence and phosphorescence, depending on the excited state. In both cases an electron has been excited from a lower energy state to a higher energy state. Afterwards the electron undergoes a radiationless transition to a lower metastable state by emission of heat. From the metastable state the electron returns to the ground state by emission a photon. The energy of the emission photon is lower than the energy of the photon that excited the electron in the first place, which results in light with a longer wavelength. A simple form of a Jablonski shown in Figure E.1 illustrates these processes. The difference between fluorescence and phosphorescence is how long time the electron stays in the metastable state. In fluorescence these

two transitions take places rapidly. A typical lifetime of fluorescence is about 10 ns. The lifetime of phosphorescence is longer and varies from milliseconds to hours depending on the material. The phenomena of phosphorescence will not be further described. [Poole and Owens, 2003]

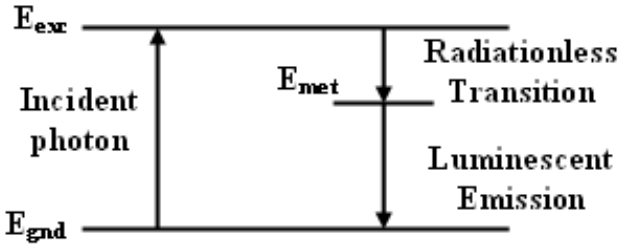

Figure E.1: *This picture illustrates the process that occurs when an excited electron returns to the ground state under emission of a photon. The radiationless transisition is released as heat.*

E.3 Fluorophores

All the molecules that can be described by the phenomena of fluorescence are called fluorophores and they are typically aromatic molecules. Some of the best known fluorophores are POPOP, Acridine Orange, and Quinine. POPOP or 1,4-bis(5-phenyloxozol-2-yl)benzene is used in scintillation counting, Acridine Orange is often used as an DNA stain and quinine is used as an antimalaria drug [Lakowicz, 1999].

The aromatic side chains of the phenylalanine (Phe), tyrosine (Tyr) and tryptophan (Trp) characterize these tree amino acids as fluorophores. These amino acids are responsible for most of the ultraviolet absorbance and fluorescence properties of protein. The side chain of Trp is the dominant of these three fluorophores and this property is often used in analysis of protein structures. The excitation intensity is most frequently between 280 and 300 nm as illustrated in Figure E.2 .

The emission of Trp varies depending on the placement in the protein. When the side chain is solvent-exposed the emission takes places at 350 nm and when the side chain is hidden inside the protein the emission takes place at 320 nm. The differences in emission make it possible to describe the concentration of Trp on the surface and inside proteins. Figure E.3 illustrates an emission spectrum of a protein containing Trp.

The purpose of fluorescence spectroscopy in this context is to study the structure of proteins and therefore analysis of fluorophores in other connections will not be further described. [Lakowicz, 1999]

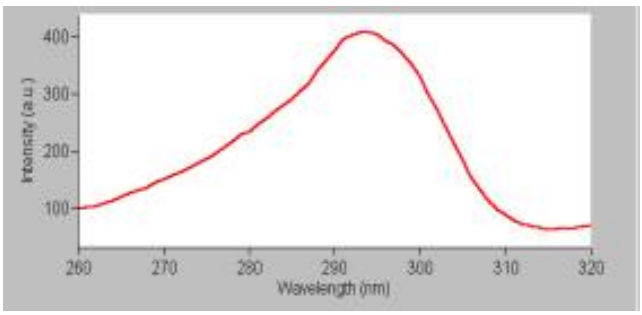

Figure E.2: *Tryptophan excitation spectra [www.varianinc.com, 2004]*

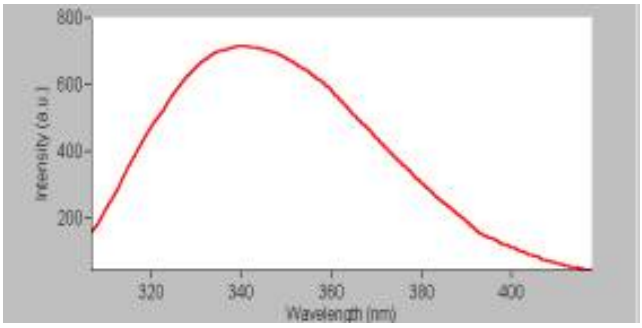

Figure E.3: *Tryptophan emission spectra [www.varianinc.com, 2004]*

E.4 Quenching

To locate the position of Trp in proteins, quenching is an important tool. By adding a quencher to a protein solution, it is possible to determine if Trp is on the surface or buried inside the protein. The principle of quenching is to decrease the intensity of the fluorescence. Quenching can be accomplished by different techniques. Collisional quenching occurs when the excited state fluorophores are inhibited by collision with another molecule in the solution. The collision makes the fluorophores return to the ground state without emission of light. The molecules are not chemical altered in the process. A wide variety of molecules can act as collisional quenchers and some examples are water, oxygen, halogens, amines and electron-deficient molecules like acrylamide. [Lakowicz, 1999]

Besides collisional quenching, fluorescence quenching can occur by other processes. Quenching can also occur as a result of the formation of a nonfluorescent complex between the fluorophore and quencher. When this complex absorbs light it immediately returns to the ground state without emission of a photon. This process is normally referred to as a static quenching since it occur in the ground state and does not rely on diffusion or molecular collisions. In proteins static quenching can be caused by disulphide bridges. Quenching can also be created by nonmolecular mechanisms such as attenuation of the light by the fluorophores itself or other

absorbing species.

In Figure E.4 it is illustrated how a quencher helps indicate the placement of Trp in a protein. The left diagram shows that adding a quencher to a protein-solvent where Trp is buried inside the protein does not affect the intensity of fluorescence. The right diagram shows how the quencher reduces the intensity of the fluorescence when Trp is placed on the surface.

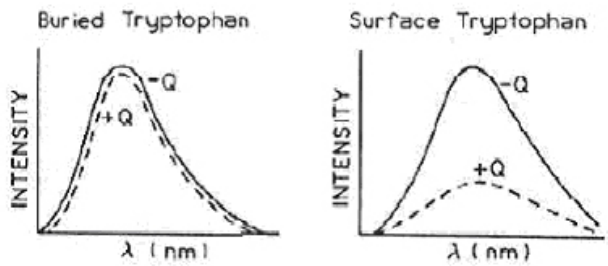

Figure E.4: *Tryptophan excitation spectra. In the left figure the quencher does not affect the intensity because Trp is buried in the center of the protein. In the right figure Trp is exposed on the surface, and the intensity is decreased.*

E.5 Thermal Unfolding

The fact that proteins denature when the temperature increases can be followed with fluorescence. The principle is to describe the stability of a protein by measuring the fluorescence intensity as a function of temperature.

A native protein, which contains Trp, can have some Trp residues buried inside the protein and some exposed on the surface, which gives the protein a specific fluorescence in the native state. Heat makes the protein denature and the buried Trp will be exposed to the solvent, which decrease the fluorescence intensity at 320 nm and increase it at 350 nm. In experiments like this it is important that the unfolding reaction have reached equilibrium before measurements are made and that the unfold reaction is reversible. The time it takes to reach equilibrium can vary from seconds to days depending on the protein and the conditions. By measuring the fluorescence intensity after the denatured protein-solution has returned to the initial temperature, it is possible to check the reversibility. Any changes in intensity will indicate that the unfolding has not been reversible. Normally thermal unfolding is not totally reversible and the reversibility is decreased the longer time the protein remains unfolded.

Proteins that contain free SH groups present special problems. The free SH groups can result in disulfide interchanges which may lead to irreversibility. If the protein contains only free SH groups and no disulfide bonds, this interaction can be avoided by adding a reducing agent such as dithiothreitol (DTT). In cases where

the protein contains free SH groups and disulfide bonds, working with low pH can reduce the interaction.

Thermophilic proteins can give some problems because the denaturation occurs at high temperatures which can be hard to reach on some spectrofluorometers. Working with low or high pH can solve this problem. By changing pH it is possible to shift the charge of the aminoacids and thereby break the salt bridges. This change in structure reduces the stability of the protein, which gives a lower denaturation temperature.

The function that describes the unfolding process is normally a S-curve, which is illustrated in Figure E.5 . The melting point (T_m) is marked on the curve in Figure E.5 and it describes the temperature where the transition is halfway.

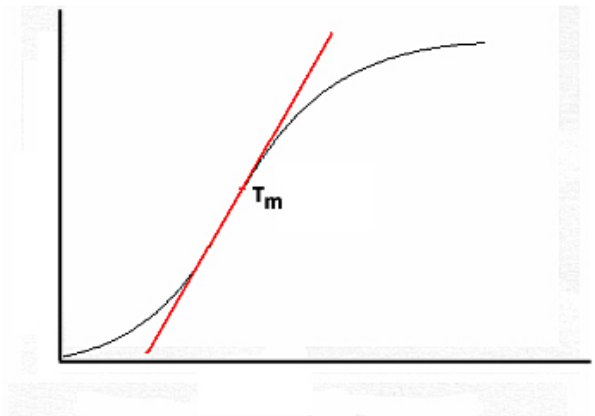

Figure E.5: *This figure shows where the T_m value is placed*

E.6 Spectrofluorometer

Figure E.6 shows that a spectrofluorometer consist of eight main parts witch are: lamp, dual grating excitation monochromator, optical module, sample chamber, emission monochromator and monochromator controller. This spectrofluorometer has a xenon lamp as the source of exciting light. This type of lamp can produce light with high intensity at all wavelengths above 250 nm. The spectrofluorometer shown in Figure E.6 is equipped with monochromators that can select the excitation and emission wavelength. The excitation monochromator contains two gratings, which minimize stray light i.e. light with wavelength different from the chosen wavelength. The optical module contains shutters, filter holder, the beam splitter and polarizers. The shutters can eliminate the exciting light or close of the emission channel. The filter holder contains a bandpass filter, which reduces the intensity of the light from the solution. This reduction is proportional to the intensity of the excitation light.

The beam splitter consists of a thin piece of quartz and reflects about 4% of the light to a reference cell. Polarizers are placed in the excitation and emission

light paths. Normally the polarizers are removable so that they can be replaced for measurements of fluorescence anisotropy or when it is necessary to select polarized components of the emission and excitation.

The sample chamber is where the samples are placed and it normally contains a heating element. The monochromator controller collects all the measurements and produces the output data [Lakowicz, 1999].

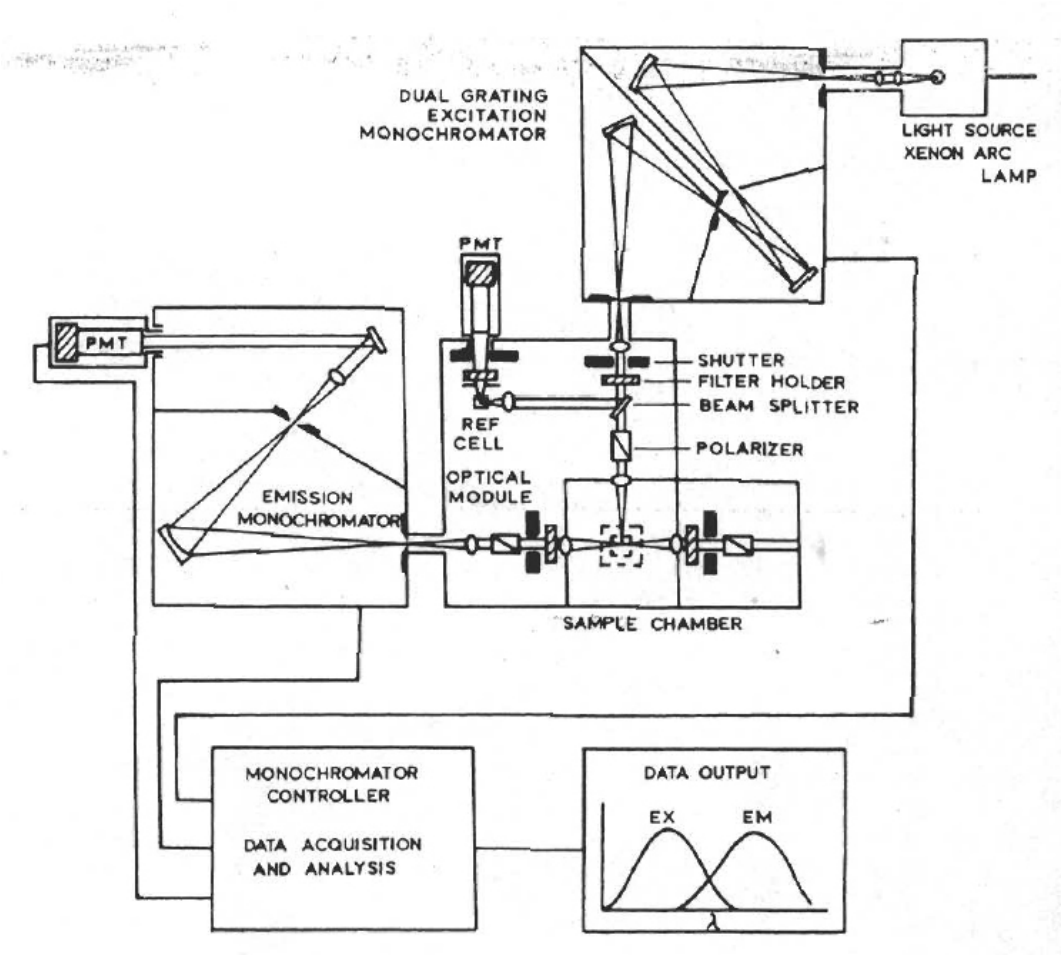

Figure E.6: *This figure is a sketch of a typical spectrofluorometer. It shows how the light travels through the device. [Lakowicz, 1999]*

Appendix F

Circular Dichroism

F.1 Principles of Circular Dichroism

Circular dichroism spectroscopy uses right and left circularly polarized light to determine the properties of the secondary structure of a protein. To do this some of the molecules in the structure must be chiral molecules, meaning that the molecule cannot cover its own mirror image. The right and left circularly polarized light are absorbed differently in the chiral molecules, which makes it possible to determine the conformation of the polymer main chain, also known as the backbone. The light used to analyze the structure, has a wavelength in the far UV-region from 190 to 250 nm [Fasman, 1996]. In a wavelength spectrum the right and left circularly polarized light is described as a function of the wavelength. This gives a graph illustrating the combinations of confirmation in the analyzed protein as seen Figure F.1 . If the solvent is heated while running the experiment, the denature process of the protein can be analyzed. When the protein is denatured by raising the temperature, the denature process is called thermal unfolding. The process of thermal unfolding happening in circular dichroism, is the same as the one described in the Appendix E .

Circularly polarized light is a wave of polarized light in a plane, for example (x,y), and a wave of polarized light in a plane orthogonal on the first, in this case (x,z). Light can be described as a wave with the wavelength λ, or a photon with a specific amount of energy. The movement of the photons following the (x,y) plane and the photon following the (x,z) plane must, in the case of circularly polarized light, have the same direction vector $\vec{e}$. From this definition the motion of circularly polarized light can be described using the unit circle assuming the wave in the (x,y) plane follows the rules of the cosine function then the top wave point will appear at zero degrees. The other wave in the (x,z) plane follows the sine function and the top wave point will appear at 90 degrees. This means that the two waves can be described trough the projection vector. The movement of this vector will either be right or left, determined by the order of the two wave top points.

To create circularly polarized light a filter is used. The filter allows only waves

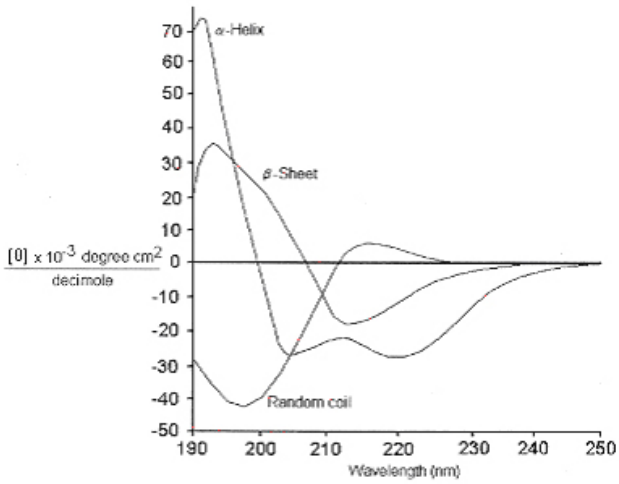

Figure F.1: *Graph of circular dichroism spectrum showing α-helices, β-sheets and random coil graphs [www.food.rdg.ac.uk/online,]*

with a specific vibration direction to pass, see Figure F.2 . The figure also shows the order of top points in right circular polarized light.

F.2 The Circular Dichroism Instrument

The circular dichroism instrument uses a high frequency photoelastic modulator to generate the two circular polarized light streams. The light is send through a variable slit size into the cuvette containing the sample. A sensor on the other side of the sample detects the light that has passed the sample. Now it is possible to calculate the absorbance, $\Delta = I_0 - I$ [Schmid, 2004]. See Figure F.3 for a simplified flowchart of the circular dichroism instrument.

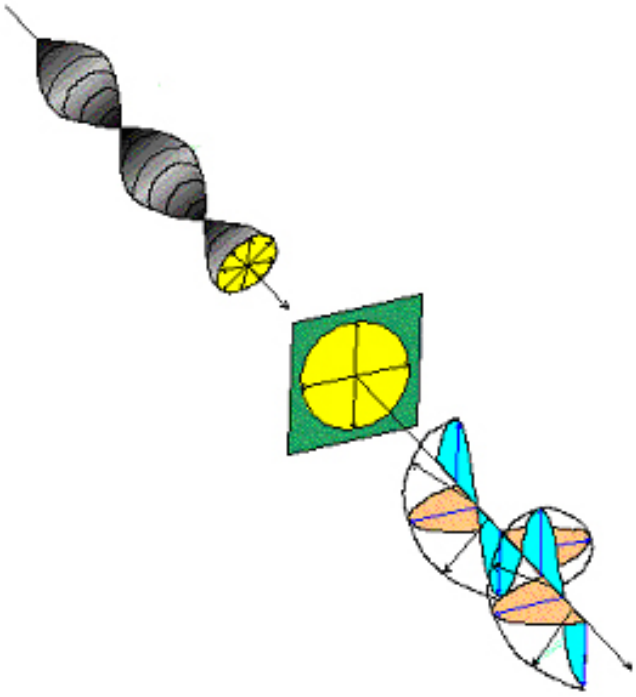

Figure F.2: *The figure shows left polarized light and how it is made using a filter. The grey "wobbling" line is normal light with waves in all directions. Modified from [www.brocku.ca, 2004]*

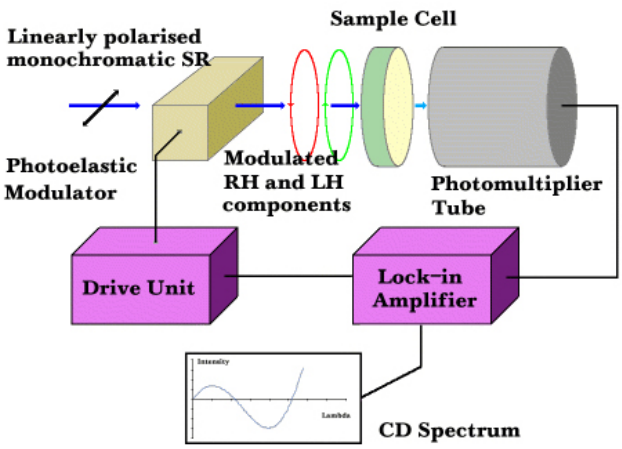

Figure F.3: *Figure showing a simplified flowchart of the CD instrument. RH and LH are right and left handed circular polarized light [www.isa.au.dk, 2004]*

Bibliography

[A303, 2004] A303, G. (2004). Group a303. Aalborg University - Faculty of Engineering and Science.

[A304, 2004] A304, G. (2004). Group a304. Aalborg University - Faculty of Engineering and Science.

[A306, 2004] A306, G. (2004). Group a306. Aalborg University - Faculty of Engineering and Science.

[A311, 2004] A311, G. (2004). Group a311. Aalborg University - Faculty of Engineering and Science.

[AAU, 2004] AAU (2004). Studievejledningen.

[Andersen et al., 1986] Andersen, E., Jespersgaard, P., and Østergaard, O. (1986). *Databogen i fysik og kemi*. F& K forlaget.

[Birdi, 2003] Birdi, K. S. (2003). *Scanning Probe Microscopy*.

[Branden and Tooze, 2003] Branden, C.-I. and Tooze, J. (2003). *Introduction to protein structure*. Garland Publishing Inc.

[Britannica, 2004] Britannica (2004). Encyclopædia britannica. Published on the World Wide Web. `www.eb.com`.

[Creighton, 1993] Creighton, T. E. (1993). *Proteins - Structures and Molecular Properties*.

[Drenth, 2002] Drenth, J. (2002). *Principles of protein X-ray crystallography*. New York, Springer.

[Encarta, 2003] Encarta (2003). *Encarta Encyclopedia*. Microsoft Corporation.

[Fasman, 1996] Fasman, G. D. (1996). *Circular Dichroism and the Conformational Analysis of Biomolecules*.

[Howland and Benatar, 2000] Howland, R. and Benatar, L. (2000). *A Practical Guide To Scanning Probe Microscopy*.

[Kittel, 1996] Kittel, C. (1996). *Introduction to solid state physics.* Wiley.

[Lademann, 2003] Lademann (2003). *Lademanns Leksikon.* Aschehoug Dansk Forlag A/S.

[Lakowicz, 1999] Lakowicz, J. R. (1999). *Principles of Fluorescence Spectroscopy.*

[Mathews, 1995] Mathews, C. K. (1995). *Biochemistry.* The Benjamin/ Cummings Publishing Company Inc.

[Mygind, 2004] Mygind, H. (2004). *Kemi 2000 B-Niveau.* Haase.

[Nielsen, 2003] Nielsen, K. H. (2003). Revolutionært eller bare hype?

[nobelprize.org, 2004] nobelprize.org (November 30th, 2004). Blue nickel. Published on the World Wide Web. `nobelprize.org/physics/educational/microscopes/scanning/gallery/8.html`.

[Nolting, 2004] Nolting, B. (2004). *Methods in Modern Biophysics.* tbd.

[Novozymes, 2004] Novozymes (November 8th, 2004). Novozymes. Published on the World Wide Web. `www.novozymes.com`.

[Poole and Owens, 2003] Poole, C. P. and Owens, F. J. (2003). *Introduction to Nanotechnology.* tbd.

[pymol.sourceforge.net, 2004] pymol.sourceforge.net (December 10th, 2004). Pymol software. `pymol.sourceforge.net`.

[Rhodes, 1993] Rhodes, G. (1993). *Crystallography made crystal clear.* Academic Press.

[Schmid, 2004] Schmid, F. X. (2004). *Optical spectroscopy to characterize protein conformation and conformational changes.*

[Serway and Beichner, 2000] Serway, R. A. and Beichner, R. J. (2000). *Physics for scientists and engineers.*

[www.brocku.ca, 2004] www.brocku.ca (December 1st, 2004). Polarization of light. Published on the World Wide Web. `www.brocku.ca/earthsciences/people/gfinn/optical/polariz1.gif`.

[www.database.iem.ac.ru, 2004] www.database.iem.ac.ru (November 24th, 2004). Crystallographic database for minerals. `www.database.iem.ac.ru/minkryst`.

[www.embl heidelberg.de, 2004] www.embl heidelberg.de (December 10th, 2004). www.embl-heidelberg.de. Published on the World Wide Web. `www.embl-heidelberg.de/~andrade/k2d.html`.

[www.food.rdg.ac.uk/online,] www.food.rdg.ac.uk/online. Secondary structure distribution. Published on the World Wide Web. www.food.rdg.ac.uk/online/fs460/lecture6/l6i.gif.

[www.isa.au.dk, 2004] www.isa.au.dk (December 1st, 2004). Cd apparatus. Published on the World Wide Web. www.isa.au.dk/SR/UV1/cds-apparatus.gif.

[www.lot oriel.it, 2004] www.lot oriel.it (December 10th, 2004). Afm for nanosurface texture/roughness. http://www.lot-oriel.com/pdf/all/pni_rough.pdf.

[www.maxon.net, 2004] www.maxon.net (December 5th, 2004). Cinema4d™. www.maxon.net.

[www.nanosurf.com, 2004] www.nanosurf.com (November 12th, 2004). *nano*surf. www.nanosurf.com.

[www.oxfordreference.com1, 2004] www.oxfordreference.com1 (November 16th, 2004). Peptide definition. Published on the World Wide Web. www.oxfordreference.com/views/ENTRY.html?subview=Main\&entry=t6.e3293.

[www.oxfordreference.com2, 2004] www.oxfordreference.com2 (November 16th, 2004). Disulphide bridges. Published on the World Wide Web. www.oxfordreference.com/views/ENTRY.html?subview=Main\&entry=t6.e1303.

[www.oxfordreference.com3, 2004] www.oxfordreference.com3 (November 16th, 2004). Salt bridges. Published on the World Wide Web. www.oxfordreference.com/views/ENTRY.html?subview=Main\&entry=t23.e49406.

[www.oxfordreference.com4, 2004] www.oxfordreference.com4 (November 17th, 2004). Proteins. Published on the World Wide Web. www.oxfordreference.com/views/ENTRY.html?subview=Main\&entry=t6.e3628.

[www.oxfordreference.com5, 2004] www.oxfordreference.com5 (November 17th, 2004). Enzymes. Published on the World Wide Web. www.oxfordreference.com/views/ENTRY.html?subview=Main\&entry=t6.e1493.

[www.people.virginia.edu, 2003] www.people.virginia.edu (November 16th, 2003). The 20 amino acids. www.people.virginia.edu/~rjh9u/aminacid.html.

[www.rcsb.org/pdb, 2004] www.rcsb.org/pdb (December 10th, 2004). Structure of hen egg-white lysozyme. www.rcsb.org/pdb/cgi/explore.cgi?pid=53491103102444\&pdbId=1DPX.

[www.rostra.dk, 2003] www.rostra.dk (December 8th, 2003). Alexander flemming, opdageren af lysozym og penicillin. Puslished on the World Wide Web. www.rostra.dk/louis/andreart/Alexander_Fleming.html.

[www.syn.aaa.dk, 2004] www.syn.aaa.dk (December 8th, 2004). Syn og lys. Published on the World Wide Web. www.syn.aaa.dk/storskriftsudgave/syn%20og%20lystekst.htm.

[www.varianinc.com, 2004] www.varianinc.com (November 6th, 2004). Tryptophan excitation. Published on the World Wide Web. www.varianinc.com/cgi-bin/nav?products/spectr/fluoro/atworks/app10&cid=OILQMJMFQ.